Sudan University of Science and Technology
College of Graduate Studies

Characterization of Brain Tumors using Magnetic Resonance Spectroscopy

توصيف اورام الدماغ باستخدام الرنين المغناطيسي الطيفي

A thesis Submitted For the Fulfillment of PhD Degree in Medical Diagnostic Radiology

By:

Ali Bashir Ali Elhag

Supervised by:

Dr. Mohamed Ahmed Ali Omer

2017

الآية

بِسْمِ اللَّهِ الرَّحْمَنِ الرَّحِيمِ

اقْرَأْ بِاسْمِ رَبِّكَ الَّذِي خَلَقَ (1) خَلَقَ الإِنسَانَ مِنْ عَلَقٍ (2) اقْرَأْ وَرَبُّكَ الأَكْرَمُ (3) الَّذِي عَلَّمَ بِالْقَلَمِ (4) عَلَّمَ الإِنسَانَ مَا لَمْ يَعْلَمْ (5) .

صَدَق اللّٰه الْعَظِيْم

سورة العلق : الآيات (1-5)

Dedication

This work is lovingly dedicated:

- *To my parents, brothers and sisters for their help and support*
- *To my Wife and my sons "Mohamed & Abobakr" for their patience, understanding and encouragement*
- *To my friends for their valuable advice*
- *To the all dearest people in my life*

Acknowledgement

- *I would like to thank ALLAH who has blessed and guided me to accomplish this thesis.*
- *I wish to express my sincerest gratitude to my supervisor* ***Dr. Mohamed Ahmed Ali Omer,*** *the Associate Professor at Sudan university of Science and Technology for his contact supervision, inexhaustible patience, constant encouragement, and for giving me a valuable times, guidance, criticism and corrections to this thesis from beginning up to end ..*
- *Moreover, I would like to thanks* ***Dr. Mohammed Abdulwahab*** *for skillful technical assistance in MRI machine and all staff in (Royal care Hospital) especially MRI department for their help and support.*

List of Contents

List of Figures

List of Tables

List of Abbreviations

Abbreviation	Full meaning
1H	Proton of stable Hydrogen-1 atom (with 1 proton and 0 neutrons)
1H-MRS	Proton Magnetic Resonance Spectroscopy
AA	Amino Acid
Ac	Acetate
ADEM	Acute Disseminated Encephalomyelitis
B0	Static external magnetic field responsible for longitudinal magnetization
CHESS	Chemical-Shift Selective
Cho	Choline
CI	Confidence Interval
Cr	Creatine
CSI	Chemical Shift Imaging
CT	Computed Tomography
DICOM	Digital Imaging and Communications in Medicine
DWI	Diffusion Weighted Imaging
Dx	Diagnosis
EBM	Evidence Based Medicine
FID	Free Induction Decay
FLAIR	FluidAttenuated Inversion Recovery
GABA	Gamma-AminobutyricAcid
GBM	Glioblastoma Multiforme
Gd	Gadolinium
Glx	Glutamine/Glutamate/GABA peak
HIE	Hypoxic-Ischaemic Encephalopathy
HIV	Human Immunodeficiency Virus
IR	Inversion Recovery
JPEG	Digital image format named after “Joint Photographic Experts Group”
Lac	Lactate
Lip	Lipid
MHz	Megahertz
MR	Magnetic Resonance
MRI	Magnetic Resonance Imaging
MRS	Magnetic Resonance Spectroscopy
MS	Multiple Sclerosis
MT	Magnetization Transfer

Mxy	Transverse magnetizationin the x-y plane
Mz	Longitudinal magnetizationin the z plane
NAA	N-acetyl aspartate
NMR	Nuclear Magnetic Resonance
NMV	Net Magnetization Vector
PACS	Picture Archiving and Communication System
PCNSL	Primary CNS Lymphoma
PD	Proton Density
PML	Progressive Multifocal Leukoencephalopathy
PNET	Primitive NeuroectodermalTumour
Ppm	Parts per million
PRESS	Point ResolvedSpectroscopy
RF	Radiofrequency
SI	Spectroscopic Imaging
S/N	Signal-to-Noise Ratio
STEAM	Stimulated Echo Acquisition Mode
Suc	Succinate
T	Tesla
T1	Time constant for longitudinal relaxation
T1w	T1 Weighted
T2	Time constant for transverse relaxation due to spin-spin energy transfer
T2*	Time constant for signal decay due inhomogeneities of external magnetic field
T2w	T2 Weighted
TE	Echo Time
TMS	Tetramethylsilane
TR	Repetition Time

Abstract

Proton spectroscopy has been recognized as a safe and non-invasive diagnostic method that coupled with MRI techniques, allows for the correlation of anatomical and physiological changes in the metabolic and biochemical processes occurring in a previously determined volume in the brain. The aim of this study was to determine the role of non-invasive technique MRS in characterization of brain tumors. Brain biopsy is invasive method, with many complication may happened during the procedure. Patient needs to be investigated by a noninvasive method with the same accuracy of the biopsy result . This study was a prospective; descriptive study of 200 patients investigated with single voxeL MR spectroscopy protocol Following routine MRI, in the period from july 2014 to july 2017 in royal care hospital in Khartoum. The data (*annual incidence, frequencies of BTs based on gender and age, anatomical location, pathologies and geographical distribution*) analyzed using EXCEL software which revealed that: : MRS showed excellent diagnostic achievement relative to standard (histology) with accuracy 86.8%BTs increase annually by a factor of 7.2% and predominant among male with 57.1%. The involved anatomical brain sites were midbrain 35%, left brain (30%) and right brain (24%). BTs observed among age groups of 1-10 years old for both gender with increasing similar trend incidence following aging which peaking at 55-65 years old. The common pathologies of brain were atrophy and infarction that represents 13.8% and 7.2% respectively and benign and malignant tumors represented (19.8%) and (34.4%) respectively. The most endemic sectors by BTs were central and Northern of Sudan that represented 45% and 35% respectively, then eastern and southern of Sudan that represented 12% and 8% respectively.MRS added to conventional MRI helps in tissue characterization of intracranial mass lesions, there by leading to an improved diagnosis of focal brain disease.

المستخلص

تم الاعتراف بالتصوير الطيفي المغنطيسي كوسيلة من وسائل التشخيص الآمنة إلى جانب تقنيات التصوير بالرنين المغناطيسي، ويسمح بارتباط التغيرات التشريحية والفسيولوجية في عمليات التمثيل الغذائي والبيو كيميائية التي تحدث في المنطقة التي سبق تحديدها في الدماغ.والهدف من هذه الدراسة لتحديد دور التصوير الطيفي المغناطيسي في توصيف أورام المخ. خزعة الدماغ هي طريقة غير امنة، مع العديد من المضاعفات قد تحدث أثناء الإجراءات. يحتاج المريض إلى فحصه بطريقة امنة وغير خطيرة بنفس كفاءة ودقة الخزعة . وكانت هذه الدراسة دراسة وصفية من 200 مريض تم تشخيصهم باستخدام بروتوكول الرنين الطيفي بعد فحص الرنين المغناطيسي الروتيني، في الفترة من يوليو 2014 إلى يوليو 2017 في مستشفى الرعاية الملكية في الخرطوم. وقد تم تحليل البيانات (معدل الإصابة السنوي، ترددات اورام المخ على أساس الجنس والعمر، والموقع التشريحي، والأمراض والتوزيع الجغرافي) باستخدام برنامج إكسيل الذي كشف أن: دقة نتائج الرنين الطيفي المغناطيسي مقارنة مع نتيجة الخزعة بلغت 86.8%اورام تزيد سنويا بنسبة 7.2٪، وتتراوح بين الذكور بنسبة 57.1٪. كانت مواقع الدماغ التشريحية المعنية وسط الدماغ 35٪، والدماغ الأيسر (30٪) والدماغ الأيمن (24٪). وقد لوحظت التراكيز بين الفئات العمرية من 1-10 سنة لكلا الجنسين مع زيادة حدوث الاتجاه مماثلة بعد الشيخوخة التي بلغت ذروتها في 55-65 سنة. وكانت الأمراض الشائعة في الدماغ ضمور واحتشاء تمثل 13.8٪ و 7.2٪ على التوالي، والأورام الحميدة ممثلة (19.8٪) والخبيثة (34.4٪) على التوالي. وكانت اكثر المناطق اصابة بأورام الدماغ هي وسط السودان التي تمثل 45٪ و وشمالي السودان 35٪ على التوالي، ثم شرق وجنوب السودان التي تمثل 12٪ و 8٪ على التوالي. اضافة الرنين الطيفي المغناطيسي إلى التصوير بالرنين المغناطيسي التقليدي يساعد في توصيف الاورام والاصابات داخل الجمجمة، مما يؤدي إلى تحسين تشخيص هذه الامراض.

Chapter One

1.1 Introduction

A tumor (also called a neoplasm or lesion) is abnormal tissue that grows by uncontrolled cell division. Normal cells grow in a controlled manner as new cells replace old or damaged ones. For reasons not fully understood, tumor cells reproduce uncontrollably. (Kabitha et al 2013). Brain tumors can occur at any age, but many types are most common in a certain age group. In adults, gliomas and meningiomas are the most common.(Pearceet al.2012).Neuroradiology plays an essential part in the clinical management of patients with brain tumors (Parizel et.al 2003).Recent technological advances have opened new windows in our ability to detect and characterize brain tumors size, site and nature (Hutter et al 2003). These new advances include Magnetic Resonance Spectroscopy (MRS) provides a non-invasive insight into the biochemistry of the brain tumor. It can offer additional diagnostic information that improves the management and outcome of patients with brain tumors (Howe et.al 2003). MR (Proton) spectroscopy has been recognized as safe and noninvasive diagnostic method that coupled with MRI techniques allows for correlation of anatomical and physiological changes in the metabolic and biochemical process occurring in previously determined volume in the brain (Kounelakis et al 2008). Diagnosis of primary and secondary brain tumors and other focal intracranial lesions based on imaging procedures alone is still challenging problem. Magnetic Resonant Spectroscopy gives completely different information related to cell membrane proliferation, neuronal damage, energy metabolism and necrotic transformation of brain or tumor tissues(Soares and Law, 2009).MRS added to conventional MRI helps in tissue characterization of intracranial mass lesions, leading to improvement in diagnosis and management of focal brain diseases (Gupta et.al 2002). Proton MRS can be used to differentiate

malignant and nonmalignant lesions from normal brain tissue and can be utilized to differentiate tumor recurrence from radiation necrosis (Magalhaes et al 2005) Malignant tumors tend to have an increased rate of membrane turnover (increased levels of choline) and a decreased concentration of neurons (decreased NAA). There are significant differences in choline/creatine ratios in relation to the tumor type with the highest values in high-grade gliomas and metastases (Fayed et.al 2005). Proton MRS may obviate the need for a brain biopsy, an invasive procedure with associated morbidity. More importantly, the method allows for the non-invasive monitoring of the response of residual tumor to therapy (Murphy et al 2005) MRS may be performed using any one of several nuclei (e.g., hydrogen, nitrogen, fluorine, phosphorus, or carbon), although MRS using hydrogen nuclei (1H MRS, proton MRS) is the predominant technique used in the brain. The method is based on the differences in resonance frequency of protons, depending on their molecular environment; this phenomenon is known as chemical shift. In proton MRS, a spectrum is generated which plots resonance frequencies on the x-axis versus amplitude (concentration) on the y-axis. Molecular compounds identified within the brain include: N-acetyl-aspartate (NAA, a neuronal marker), choline (a cell membrane marker), creatine and phosphocreatine (energy metabolites), and lactate (a by-product of cerebral metabolism). Proton MRS is helpful in the characterization of brain tumors (Magalhaes et al 2005).

1.2 Problem of the study

Brain biopsy is invasive method, with many complication may happened during the procedure. Patient needs to be investigated by a noninvasive method with the same accuracy of the biopsy result. MRS is a new imaging noninvasive technique used in MRI examination and the accuracy of MRS needs to be tested for brain tumors characterization.

1.3 Objectives of the study

1.3.1 General objective

To characterize brain tumors using magnetic resonance spectroscopy (MRS)

1.3.2 Specific objective

- To find out the accuracy of MRS in brain tumors.
- To measure the incidence of brain tumors and account for frequency
- To determine the most location of tumors in brain
- To detect the distribution of brain tumors in different geographical sectors of Sudan
- To detect the types of brain pathologies in Sudanese population
- To correlate all the finding with patient age , gender and chemical signs

1.4 Significance of the study

This study will provide a Sudanese index (dimension) for brain tumors.

1.5 Overview of the study

The skeleton of thesis is built upon five chapters. Chapter one is consist of introduction, problem of the study, general, specific objectives and significant of the study. Chapter two concerns with Literature review. Chapter three is about the methodology which includes material and method, chapter four about the result presentation, chapter five about the discussion, conclusion, recommendation and limitations including the references and appendixes.

Chapter Two

Literature review

2.1 Anatomy of the Brain

The brain is an amazing three-pound organ that controls all functions of the body, interprets information from the outside world, and embodies the essence of the mind and soul. Intelligence, creativity, emotion, and memory are a few of the many things governed by the brain. Protected within the skull, the brain is composed of the cerebrum, cerebellum, and brainstem. The brainstem acts as a relay center connecting the cerebrum and cerebellum to the spinal cord .The brain receives information through our five senses: sight, smell, touch, taste, and hearing - often many at one time. It assembles the messages in a way that has meaning for us, and can store that information in our memory. The brain controls our thoughts, memory and speech, movement of the arms and legs, and the function of many organs within our body. It also determines how we respond to stressful situations (such as taking a test, losing a job, or suffering an illness) by regulating our heart and breathing rate (Heimer et al 2012).

2.1.1 Nervous system

The nervous system is divided into central and peripheral systems. The central nervous system (CNS) is composed of the brain and spinal cord. The peripheral nervous system (PNS) is composed of spinal nerves that branch from the spinal cord and cranial nerves that branch from the brain. The PNS includes the autonomic nervous system, which controls vital functions such as breathing, digestion, heart rate, and secretion of hormones (Heimer et al 2012).

2.1.2 Skull

The purpose of the bony skull is to protect the brain from injury. The skull is formed from 8 bones that fuse together along suture lines. These bones include the frontal, parietal (2), temporal (2), sphenoid, occipital and ethmoid (Fig. 1). The face is formed from 14 paired bones including the maxilla, zygoma, nasal, palatine, lacrimal, inferior nasal conchae, mandible, and vomer (Norton, Neil 2016).

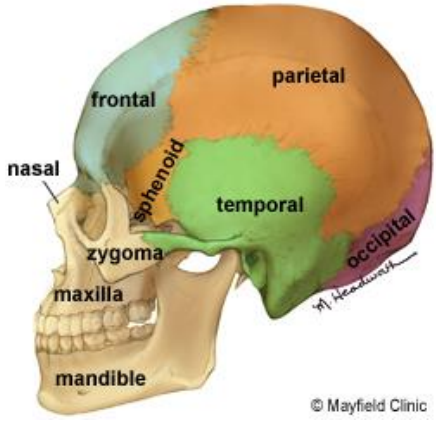

Figure 1. Eight bones form the skull and fourteen bones form the face.(Mayfield Brain & Spine 2016)

Inside the skull are three distinct areas: anterior fossa, middle fossa, and posterior fossa (Fig. 2). Doctors sometimes refer to a tumor's location by these terms, e.g., middle fossa meningioma.

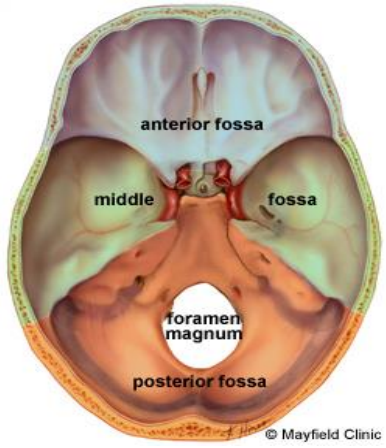

Figure 2. The inside of the skull is divided into three areas called the anterior, middle, and posterior fossae. (Mayfield Brain & Spine 2016).

Similar to cables coming out the back of a computer, all the arteries, veins and nerves exit the base of the skull through holes, called foramina. The big hole in the middle (foramen magnum) is where the spinal cord exits.

2.1.3 Brain

The brain is composed of the cerebrum, cerebellum, and brainstem (Fig. 3).

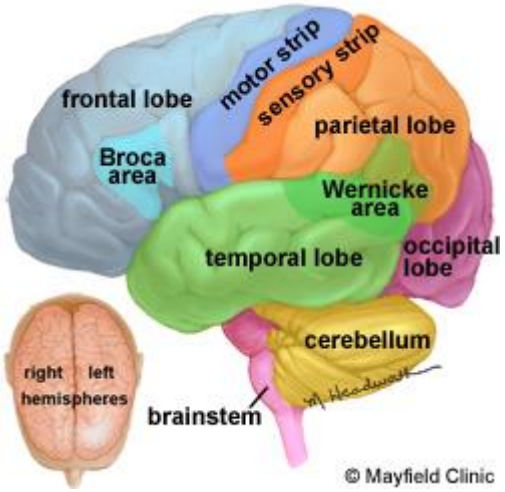

Figure 3. The brain is composed of three parts: the brainstem, cerebellum, and cerebrum. The cerebrum is divided into four lobes: frontal, parietal, temporal, and occipital. (Mayfield Brain & Spine 2016)

The cerebrum is the largest part of the brain and is composed of right and left hemispheres. It performs higher functions like interpreting touch, vision and hearing, as well as speech, reasoning, emotions, learning, and fine control of movement.The cerebellum is located under the cerebrum. Its function is to coordinate muscle movements, maintain posture and balance.
The brainstem includes the midbrain, pons, and medulla. It acts as a relay center connecting the cerebrum and cerebellum to the spinal cord. It performs many automatic functions such as breathing, heart rate, body temperature, wake and sleep cycles, digestion, sneezing, coughing, vomiting, and swallowing. Ten of the twelve cranial nerves originate in the brainstem.The surface of the cerebrum has a

folded appearance called the cortex. The cortex contains about 70% of the 100 billion nerve cells. The nerve cell bodies color the cortex grey-brown giving it its name – gray matter (Fig. 4). Beneath the cortex are long connecting fibers between neurons, called axons, which make up the white matter.

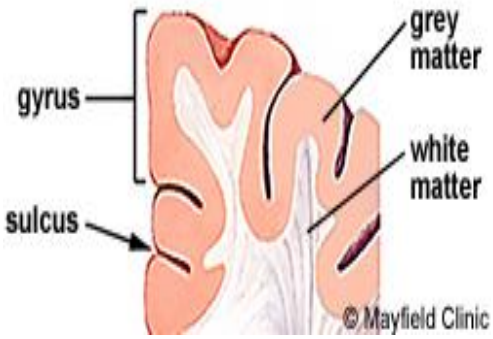

Figure 4. The surface of the cerebrum is called the cortex. The cortex contains neurons (grey matter), which are interconnected to other brain areas by axons (white matter). The cortex has a folded appearance. A fold is called a gyrus and the groove between is a sulcus. .(Mayfield Brain & Spine 2016*)*

The folding of the cortex increases the brain's surface area allowing more neurons to fit inside the skull and enabling higher functions. Each fold is called a gyrus, and each groove between folds is called a sulcus. There are names for the folds and grooves that help define specific brain regions (Fehrenbach et al 2015).

2.1.3.1 Right brain – left brain

The right and left hemispheres of the brain are joined by a bundle of fibers called the corpus callosum that delivers messages from one side to the other. Each hemisphere controls the opposite side of the body. If a brain tumor is located on the right side of the brain, your left arm or leg may be weak or paralyzed.

Not all functions of the hemispheres are shared. In general, the left hemisphere controls speech, comprehension, arithmetic, and writing. The right hemisphere controls creativity, spatial ability, artistic, and musical skills. The left hemisphere

is dominant in hand use and language in about 92% of people(Fehrenbach et al 2015).

2.1.3.2 Lobes of the brain

The cerebral hemispheres have distinct fissures, which divide the brain into lobes. Each hemisphere has 4 lobes: frontal, temporal, parietal, and occipital (Fig 3). Each lobe may be divided, once again, into areas that serve very specific functions. It's important to understand that each lobe of the brain does not function alone. There are very complex relationships between the lobes of the brain and between the right and left hemispheres(Fehrenbach et al 2015).

2.1.3.2.1 Frontal lobe

- Personality, behavior, emotions
- Judgment, planning, problem solving
- Speech: speaking and writing (Broca's area)
- Body movement (motor strip)
- Intelligence, concentration, self awareness

2.1.3.2.2 Parietal lobe

- Interprets language, words
- Sense of touch, pain, temperature (sensory strip)
- Interprets signals from vision, hearing, motor, sensory and memory
- Spatial and visual perception

2.1.3.2.3 Occipital lobe

- Interprets vision (color, light, movement)

2.1.3.2.4 Temporal lobe

- Understanding language (Wernicke's area)
- Memory

- Hearing
- Sequencing and organization

Messages within the brain are carried along pathways. Messages can travel from one gyrus to another, from one lobe to another, from one side of the brain to the other, and to structures found deep in the brain (e.g. thalamus, hypothalamus) (Fehrenbach et al 2015).

2.1.3.3 Deep structures:

Hypothalamus - is located in the floor of the third ventricle and is the master control of the autonomic system. It plays a role in controlling behaviors such as hunger, thirst, sleep, and sexual response. It also regulates body temperature, blood pressure, emotions, and secretion of hormones.

Pituitary gland - lies in a small pocket of bone at the skull base called the sella turcica. The pituitary gland is connected to the hypothalamus of the brain by the pituitary stalk. Known as the "master gland," it controls other endocrine glands in the body. It secretes hormones that control sexual development, promote bone and muscle growth, respond to stress, and fight disease.

Pineal gland - is located behind the third ventricle. It helps regulate the body's internal clock and circadian rhythms by secreting melatonin. It has some role in sexual development(Fehrenbach et al 2015).

Thalamus - serves as a relay station for almost all information that comes and goes to the cortex (Fig. 5). It plays a role in pain sensation, attention, alertness and memory.

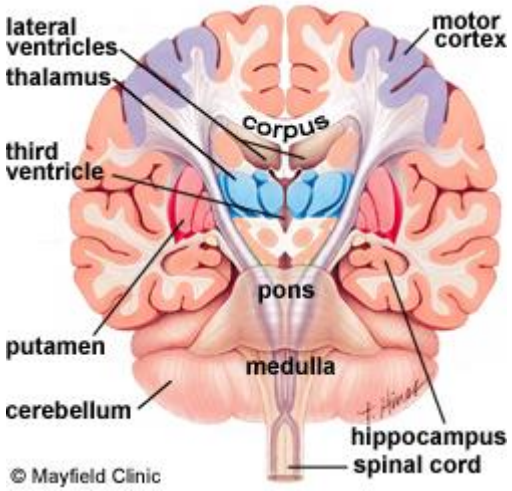

Figure 5. Coronal cross-section showing the basal ganglia. .(Mayfield Brain & Spine 2016)

Basal ganglia - includes the caudate, putamen and globus pallidus. These nuclei work with the cerebellum to coordinate fine motions, such as fingertip movements.

Limbic system - is the center of our emotions, learning, and memory. Included in this system are the cingulate gyri, hypothalamus, amygdala (emotional reactions) and hippocampus (memory) (Fehrenbach, Margaret 2015).

2.1.3.4 Cranial nerves

The brain communicates with the body through the spinal cord and twelve pairs of cranial nerves (Fig. 6). Ten of the twelve pairs of cranial nerves that control hearing, eye movement, facial sensations, taste, swallowing and movement of the face, neck, shoulder and tongue muscles originate in the brainstem. The cranial nerves for smell and vision originate in the cerebrum (Heimer, Lennart 2012).

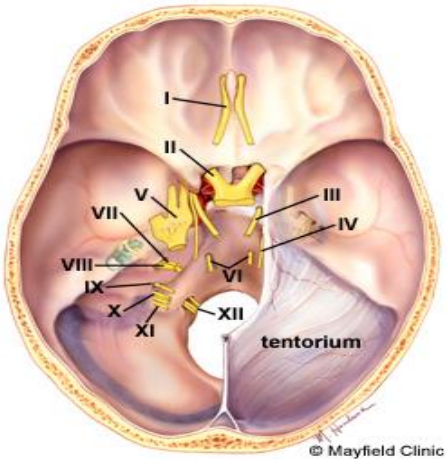

Figure 6. The Roman numeral, name, and main function of the twelve cranial nerves. .(Mayfield Brain & Spine 2016)

Table 2-1 cranial nerve

Number	Name	Function
I	Olfactory	Smell
II	Optic	Sight
III	Oculomotor	moves eye, pupil
IV	Trochlear	moves eye
V	Trigeminal	face sensation
VI	Abducens	moves eye
VII	Facial	moves face, salivate
VIII	vestibulocochlear	hearing, balance
IX	glossopharyngeal	taste, swallow
X	Vagus	heart rate, digestion
XI	Accessory	moves head
XII	Hypoglossal	moves tongue

2.1.3.5 Meninges

The brain and spinal cord are covered and protected by three layers of tissue called meninges. From the outermost layer inward they are: the dura mater, arachnoid mater, and pia mater.

The dura mater is a strong, thick membrane that closely lines the inside of the skull; its two layers, the periosteal and meningeal dura, are fused and separate only to form venous sinuses. The dura creates little folds or compartments. There are two special dural folds, the falx and the tentorium. The falx separates the right and left hemispheres of the brain and the tentorium separates the cerebrum from the cerebellum.

The arachnoid mater is a thin, web-like membrane that covers the entire brain. The arachnoid is made of elastic tissue. The space between the dura and arachnoid membranes is called the subdural space.

The pia mater hugs the surface of the brain following its folds and grooves. The pia mater has many blood vessels that reach deep into the brain. The space between the arachnoid and pia is called the subarachnoid space. It is here where the cerebrospinal fluid bathes and cushions the brain(Heimer, Lennart 2012).

2.1.3.6 Ventricles and cerebrospinal fluid

The brain has hollow fluid-filled cavities called ventricles (Fig. 7). Inside the ventricles is a ribbon-like structure called the choroid plexus that makes clear colorless cerebrospinal fluid (CSF). CSF flows within and around the brain and spinal cord to help cushion it from injury. This circulating fluid is constantly being absorbed and replenished.

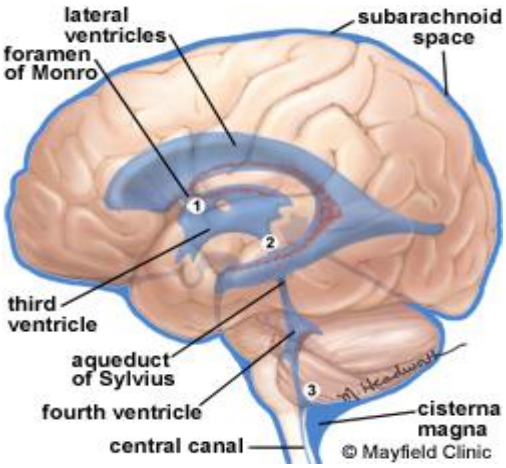

Figure 7. CSF is produced inside the ventricles deep within the brain. CSF fluid circulates inside the brain and spinal cord and then outside to the subarachnoid space. Common sites of obstruction: 1) foramen of Monro, 2) aqueduct of Sylvius, and 3) obex.(Mayfield Brain & Spine 2016)

There are two ventricles deep within the cerebral hemispheres called the lateral ventricles. They both connect with the third ventricle through a separate opening called the foramen of Monro. The third ventricle connects with the fourth ventricle through a long narrow tube called the aqueduct of Sylvius. From the fourth ventricle, CSF flows into the subarachnoid space where it bathes and cushions the brain. CSF is recycled (or absorbed) by special structures in the superior sagittal sinus called arachnoid villi.

A balance is maintained between the amount of CSF that is absorbed and the amount that is produced. A disruption or blockage in the system can cause a build up of CSF, which can cause enlargement of the ventricles (hydrocephalus) or cause a collection of fluid in the spinal cord (syringomyelia) (Heimer, Lennart 2012).

2.1.3.7 Blood supply

Blood is carried to the brain by two paired arteries, the internal carotid arteries and the vertebral arteries (Fig. 8). The internal carotid arteries supply most of the cerebrum.

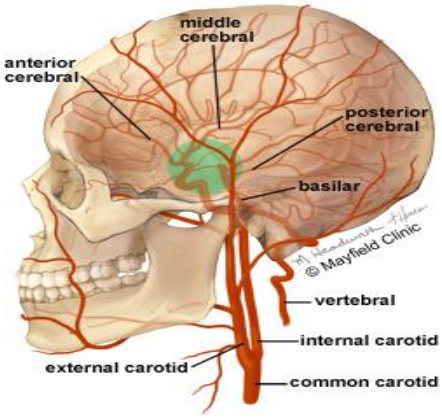

Figure 8. The common carotid artery courses up the neck and divides into the internal and external carotid arteries. The brain's anterior circulation is fed by the internal carotid arteries (ICA) and the posterior circulation is fed by the vertebral arteries (VA). The two systems connect at the Circle of Willis (green circle). .(Mayfield Brain & Spine 2016)

The vertebral arteries supply the cerebellum, brainstem, and the underside of the cerebrum. After passing through the skull, the right and left vertebral arteries join together to form the basilar artery. The basilar artery and the internal carotid arteries "communicate" with each other at the base of the brain called the Circle of Willis (Fig. 9). The communication between the internal carotid and vertebral-basilar systems is an important safety feature of the brain. If one of the major vessels becomes blocked, it is possible for collateral blood flow to come across the Circle of Willis and prevent brain damage (Heimer, Lennart 2012).

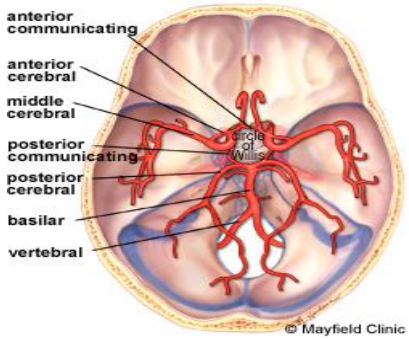

Figure 9. Top view of the Circle of Willis. The internal carotid and vertebral-basilar systems are joined by the anterior communicating and posterior communicating arteries. .(Mayfield Brain & Spine 2016)

The venous circulation of the brain is very different from that of the rest of the body. Usually arteries and veins run together as they supply and drain specific areas of the body. So one would think there would be a pair of vertebral veins and internal carotid veins. However, this is not the case in the brain. The major vein collectors are integrated into the dura to form venous sinuses (Fig. 10) - not to be confused with the air sinuses in the face and nasal region. The venous sinuses collect the blood from the brain and pass it to the internal jugular veins. The superior and inferior sagittal sinuses drain the cerebrum, the cavernous sinuses drains the anterior skull base. All sinuses eventually drain to the sigmoid sinuses, which exit the skull and form the jugular veins. These two jugular veins are essentially the only drainage of the brain(Fehrenbach et al 2015).

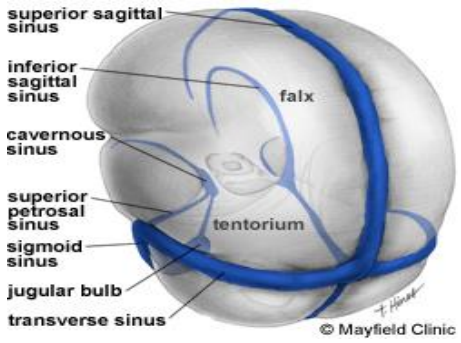

Figure 10. Three quarter view of the dural covering of the brain depicts the two major dural folds, the falx and tentorium along with the venous sinuses. (Mayfield Brain & Spine 2016)

2.1.3.8 Language

In general, the left hemisphere of the brain is responsible for language and speech and is called the "dominant" hemisphere. The right hemisphere plays a large part in interpreting visual information and spatial processing. In about one third of individuals who are left-handed, speech function may be located on the right side of the brain. Left-handed individuals may need special testing to determine if their speech center is on the left or right side prior to any surgery in that area.

Aphasia is a disturbance of language affecting production, comprehension, reading or writing, due to brain injury – most commonly from stroke or trauma. The type of aphasia depends on the brain area affected (Fehrenbach, Margaret 2015)..

2.1.3.8.1 Broca's area

lies in the left frontal lobe (Fig 3). If this area is damaged, one may have difficulty moving the tongue or facial muscles to produce the sounds of speech. The individual can still read and understand spoken language but has difficulty in speaking and writing (i.e. forming letters and words, doesn't write within lines) – called Broca's aphasia.

2.1.3.8.2 Wernicke's area

lies in the left temporal lobe (Fig 3). Damage to this area causes Wernicke's aphasia. The individual may speak in long sentences that have no meaning, add unnecessary words, and even create new words. They can make speech sounds, however they have difficulty understanding speech and are therefore unaware of their mistakes.

2.1.3.9 Memory

Memory is a complex process that includes three phases: encoding (deciding what information is important), storing, and recalling. Different areas of the brain are involved in memory depending on the type of memory.

*Short-term memory, also called working memory, occurs in the prefrontal cortex. It stores information for about one minute and its capacity is limited to about 7 items. For example, it enables you to dial a phone number someone just told you. It also intervenes during reading, to memorize the sentence you have just read, so that the next one makes sense.

*Long-term memory is processed in the hippocampus of the temporal lobe and is activated when you want to memorize something for a longer time. This memory has unlimited content and duration capacity. It contains personal memories as well as facts and figures.

*Skill memory is processed in the cerebellum, which relays information to the basal ganglia. It stores automatic learned memories like tying a shoe, playing an instrument, or riding a bike.

2.1.3.10 Cells of the brain

The brain is made up of two types of cells: nerve cells (neurons) and glia cells.

2.1.3.10.1 Nerve cells

There are many sizes and shapes of neurons, but all consist of a cell body, dendrites and an axon. The neuron conveys information through electrical and chemical signals. Try to picture electrical wiring in your home. An electrical circuit is made up of numerous wires connected in such a way that when a light switch is turned on, a light bulb will beam. A neuron that is excited will transmit its energy to neurons within its vicinity.

Neurons transmit their energy, or “talk”, to each other across a tiny gap called a synapse (Fig. 11). A neuron has many arms called dendrites, which act like antennae picking up messages from other nerve cells. These messages are passed to the cell body, which determines if the message should be passed along. Important messages are passed to the end of the axon where sacs containing neurotransmitters open into the synapse. The neurotransmitter molecules cross the synapse and fit into special receptors on the receiving nerve cell, which stimulates that cell to pass on the message.

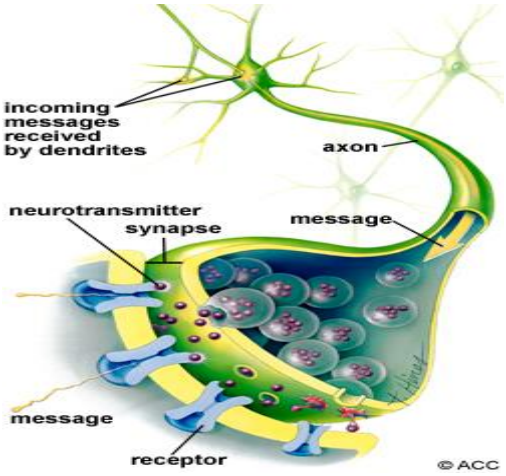

Figure 11. Nerve cells consist of a cell body, dendrites and axon. Neurons communicate with each other by exchanging neurotransmitters across a tiny gap called a synapse.Glia cells . (Mayfield Brain & Spine 2016).

Glia (Greek word meaning glue) are the cells of the brain that provide neurons with nourishment, protection, and structural support. There are about 10 to 50 times more glia than nerve cells and are the most common type of cells involved in brain tumors.

1 -Astroglia

or astrocytes transport nutrients to neurons, hold neurons in place, digest parts of dead neurons, and regulate the blood brain barrier.

2- Oligodendroglia

Cells provide insulation (myelin) to neurons.

3 -Ependymal

Cells line the ventricles and secrete cerebrospinal fluid (CSF).

4 -Microglia

Digest dead neurons and pathogens(Fehrenbach, Margaret J 2015)..

2.2 Brain Tumors

A brain tumor, known as an intracranial tumor, is an abnormal mass of tissue in which cells grow and multiply uncontrollably, seemingly unchecked by the mechanisms that control normal cells. More than 150 different brain tumors have been documented, but the two main groups of brain tumors are termed primary and metastatic (Kwabi-Addo et.al 2011).

Primary brain tumors include tumors that originate from the tissues of the brain or the brain's immediate surroundings. Primary tumors are categorized as glial (composed of glial cells) or non-glial (developed on or in the structures of the brain, including nerves, blood vessels and glands) and benign or malignant (Kwabi-Addo et.al 2011).

Metastatic brain tumors include tumors that arise elsewhere in the body (such as the breast or lungs) and migrate to the brain, usually through the bloodstream. Metastatic tumors are considered cancer and are malignant. Metastatic tumors to the brain affect nearly one in four patients with cancer, or an estimated 150,000 people a year. Up to 40 percent of people with lung cancer will develop metastatic brain tumors. In the past, the outcome for patients diagnosed with these tumors was very poor, with typical survival rates of just several weeks. More sophisticated diagnostic tools, in addition to innovative surgical and radiation approaches, have helped survival rates expand up to years; and also allowed for an improved quality of life for patients following diagnosis(Kwabi-Addo et.al 2011).

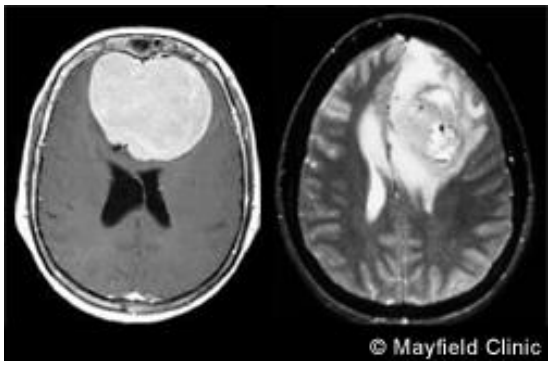

Figure 12. MRI scans of a benign and malignant brain tumor. Benign tumors have well defined edges and are more easily removed surgically. Malignant tumors have an irregular border that invades normal tissue with finger-like projections making surgical removal more difficult.

2.2.1 Types of Benign Brain Tumors

2.2.1.1 Chordomas are benign, slow-growing tumors that are most prevalent in people ages 50 to 60. Their most common locations are the base of the skull and the lower portion of the spine. Although these tumors are benign, they may invade the adjacent bone and put pressure on nearby neural tissue. These are rare tumors, contributing to only 0.2 percent of all primary brain tumors (Bosc, Romain et.al 2011).

2.2.1.2 Craniopharyngiomas typically are benign, but are difficult tumors to remove because of their location near critical structures deep in the brain. They usually arise from a portion of the pituitary gland (the structure that regulates many hormones in the body), so nearly all patients will require some hormone replacement therapy(Bosc et.al 2011).

2.2.1.3 Gangliocytomas, gangliomas and anaplastic gangliogliomas are rare tumors that include neoplastic nerve cells that are relatively well-differentiated, occurring primarily in young adults (Bosc et.al 2011).

2.2.1.4 Glomus jugulare tumors most frequently are benign and typically are located just under the skull base, at the top of the jugular vein. They are the most common form of glomus tumor. However, glomus tumors, in general, contribute to only 0.6 percent of neoplasms of the head and neck(Bosc et.al 2011).

2.2.1.5 Meningiomas are the most common benign intracranial tumors, comprising 10 to 15 percent of all brain neoplasms, although a very small percentage are malignant. These tumors originate from the meninges, the membrane-like structures that surround the brain and spinal cord (Bosc et.al 2011).

2.2.1.6 Pineocytomas are generally benign lesions that arise from the pineal cells, occurring predominantly in adults. They are most often well-defined, noninvasive, homogeneous and slow-growing (Bosc et.al 2011).

2.2.1.7 Pituitary adenomas are the most common intracranial tumors after gliomas, meningiomas and schwannomas. The large majority of pituitary adenomas are benign and fairly slow-growing. Even malignant pituitary tumors rarely spread to other parts of the body. Adenomas are by far the most common disease affecting the pituitary. They commonly affect people in their 30s or 40s, although they are diagnosed in children, as well. Most of these tumors can be treated successfully (Bosc et.al 2011).

2.2.1.8 Schwannomas are common benign brain tumors in adults. They arise along nerves, comprised of cells that normally provide the "electrical insulation" for the nerve cells. Schwannomas often displace the remainder of the normal nerve instead of invading it. Acoustic neuromas are the most common schwannoma, arising from the eighth cranial nerve, or vestibular cochlear nerve, which travels from the brain to the ear. Although these tumors are benign, they can cause serious complications and even death if they grow and exert pressure on nerves and

eventually on the brain. Other locations include the spine and, more rarely, along nerves that go to the limbs (Bosc et.al 2011).

2.2.2 Types of Malignant Brain Tumors

2.2.2.1 Gliomas are the most prevalent type of adult brain tumor, accounting for 78 percent of malignant brain tumors. They arise from the supporting cells of the brain, called the glia. These cells are subdivided into astrocytes, ependymal cells and oligodendroglial cells (or oligos). Glial tumors include the following:

2.2.2.2 Astrocytomas are the most common glioma, accounting for about half of all primary brain and spinal cord tumors. Astrocytomas develop from star-shaped glial cells called astrocytes, part of the supportive tissue of the brain. They may occur in many parts of the brain, but most commonly in the cerebrum. People of all ages can develop astrocytomas, but they are more prevalent in adults — particularly middle-aged men. Astrocytomas in the base of the brain are more prevalent in children n or younger people and account for the majority of children's brain tumors. In children, most of these tumors are considered low-grade, while in adults, most are high-grade.

2.2.2.3 Ependymomas are derived from a neoplastic transformation of the ependymal cells lining the ventricular system and account for two to three percent of all brain tumors. Most are well-defined, but some are not.

2.2.2.4 Glioblastoma multiforme (GBM) is the most invasive type of glial tumor. These tumors tend to grow rapidly, spread to other tissue and have a poor prognosis. They may be composed of several different kinds of cells, such as astrocytes and oligodendrocytes. GBM is more common in people ages 50 to 70 and are more prevalent in men than women.

2.2.2.5 Medulloblastomas usually arise in the cerebellum, most frequently in children. They are high-grade tumors, but they are usually responsive to radiation and chemotherapy.

2.2.2.6 Oligodendrogliomas are derived from the cells that make myelin, which is the insulation for the wiring of the brain(Bosc et.al 2011).

2.2.3 Other Types of Brain Tumors

2.2.3.1 Hemangioblastomas are slow-growing tumors, commonly located in the cerebellum. They originate from blood vessels, can be large in size and often are accompanied by a cyst. These tumors are most common in people ages 40 to 60 and are more prevalent in men than women (Nandigam et.al 2014).

2.2.3.2 Rhabdoid tumors are rare, highly aggressive tumors that tend to spread throughout the central nervous system. They often appear in multiple sites in the body, especially in the kidneys. They are more prevalent in young children, but also can occur in adults (Nandigam et.al 2014).

2.2.4 Pediatric Brain Tumors

Brain tumors in children typically come from different tissues than those affecting adults. Treatments that are fairly well-tolerated by the adult brain (such as radiation therapy) may prevent normal development of a child's brain, especially in children younger than age five (Tobin et al 2015).

According to the Pediatric Brain Tumor Foundation, approximately 4,200 children are diagnosed with a brain tumor in the U.S. Seventy-two percent of children diagnosed with a brain tumor are younger than age 15. In some patients the descended cerebellar components are debulked or removed.

Some types of brain tumors are more common in children than in adults. The most common types of pediatric tumors are medulloblastomas, low-grade astrocytomas

(pilocytic), ependymomas, craniopharyngiomas and brainstem gliomas (Tobin et al 2015).

2.2.5 World Health Organization (WHO) Brain Tumor Grades

The World Health Organization (WHO) has developed a grading system to indicate a tumor's malignancy or benignity based on its histological features under a microscope:

1- Most malignant

2- Rapid growth, aggressive

3- Widely infiltrative

4- Rapid recurrence

5- Necrosis prone

Table 2: World Health Organization (WHO) Brain Tumor Grades (Louis et al. 2016.)

	Grade	Characteristics	Tumor Types
Low Grade	WHO Grade I	• Least malignant (benign) • Possibly curable via surgery alone • Non-infiltrative • Long-term survival • Slow growing	• Pilocytic astrocytoma • Craniopharyngioma • Gangliocytoma • Ganglioglioma •
	WHO Grade II	• Relatively slow growing • Somewhat infiltrative • May recur as higher grade	• "Diffuse" Astrocytoma • Pineocytoma • Pure oligodendroglioma •
High Grade	WHO Grade III	• Malignant • Infiltrative • Tend to recur as higher grade	• Anaplastic astrocytoma • Anaplastic ependymoma • Anaplastic oligodendroglioma
	WHO Grade IV	• Most malignant • Raid growth, aggressive • Widely infiltrative • Rapid recurrence • Necrosis prone	• Gliobastoma multiforme (GBM) • Pineoblastoma • Medulloblastoma • Ependymoblastoma

2.2.6 Incidence in Adults

The National Cancer Institute estimates that 22,910 adults (12,630 men and 10,280 women) will be diagnosed with brain and other nervous system tumors in 2012. It also estimates that in 2012, 13,700 of these diagnoses will result in death.Between 2005 and 2009, the median age for death from cancer of the brain and other areas of the nervous system was age 64(Horner et al 2009).

2.2.7 Brain Tumor Causes

Brain tumors are thought to arise when certain genes on the chromosomes of a cell are damaged and no longer function properly. These genes normally regulate the rate at which the cell divides (if it divides at all) and repair genes that fix defects of other genes, as well as genes that should cause the cell to self-destruct if the damage is beyond repair. In some cases, an individual may be born with partial defects in one or more of these genes. Environmental factors may then lead to further damage. In other cases, the environmental injury to the genes may be the only cause. It is not known why some people in an "environment" develop brain tumors, while others do not (Schneider and Katherine 2011).

Once a cell is dividing rapidly and internal mechanisms to check its growth are damaged, the cell can eventually grow into a tumor. Another line of defense may be the body's immune system, which optimally would detect the abnormal cell and kill it. Tumors may produce substances that block the immune system from recognizing the abnormal tumor cells and eventually overpower all internal and external deterrents to its growth (Schneider and Katherine 2011).

A rapidly growing tumor may need more oxygen and nutrients than can be provided by the local blood supply intended for normal tissue. Tumors can produce substances called angiogenesis factors that promote the growth of blood vessels.

The new vessels that grow increase the supply of nutrients to the tumor, and, eventually, the tumor becomes dependent on these new vessels. Research is being done in this area, but more extensive research is necessary to translate this knowledge into potential therapies (Schneider and Katherine 2011).

2.2.8 Symptoms

Symptoms vary depending on the location of the brain tumor, but the following may accompany different types of brain tumor:

1- Headaches that may be more severe in the morning or awaken the patient at night

2- Seizures or convulsions

3- Difficulty thinking, speaking or articulating

4- Personality changes

5- Weakness or paralysis in one part or one side of the body

6- Loss of balance or dizziness

7- Vision changes

8- Hearing changes

9- Facial numbness or tingling

10- Nausea or vomiting, swallowing difficulties

11- Confusion and disorientation (Siegel, Rebecca L et.al 2015)

2.2.9 Diagnosis

Sophisticated imaging techniques can pinpoint brain tumors. Diagnostic tools include computed tomography (CT or CAT scan) and magnetic resonance imaging (MRI). Other MRI sequences can help the surgeon plan the resection of the tumor based on the location of the normal nerve pathways of the brain. Intraoperative MRI also is used during surgery to guide tissue biopsies and tumor removal. Magnetic resonance spectroscopy (MRS) is used to examine the tumor's chemical

profile and determine the nature of the lesions seen on the MRI. Positron emission tomography (PET scan) can help detect recurring brain tumors.

Sometimes the only way to make a definitive diagnosis of a brain tumor is through a biopsy. The neurosurgeon performs the biopsy and the pathologist makes the final diagnosis, determining whether the tumor appears benign or malignant, and grading it accordingly.

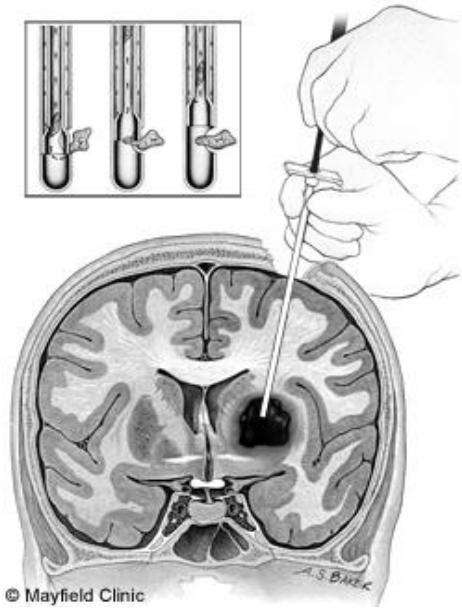

Figure 13. During a needle biopsy, a hollow cannula is inserted into the tumor. Small biting instruments remove bits of tumor for the pathologist to examine and determine the exact tumor cell type.

2.2.10 Brain Tumor Treatment

Brain tumors (whether primary or metastatic, benign or malignant) usually are treated with surgery, radiation, and/or chemotherapy — alone or in various combinations. While it is true that radiation and chemotherapy are used more often for malignant, residual or recurrent tumors, decisions as to what treatment to use are made on a case-by-case basis and depend on a number of factors. There are risks and side effects associated with each type of therapy(Buckner et a 2007).

2.2.10.1 Surgery

It is generally accepted that complete or nearly complete surgical removal of a brain tumor is beneficial for a patient. The neurosurgeon's challenge is to remove as much tumor as possible, without injuring brain tissue important to the patient's neurological function (such as the ability to speak, walk, etc.). Traditionally, neurosurgeons open the skull through a craniotomy to insure they can access the tumor and remove as much of it as possible. A drain (EVD) may be left in the brain fluid cavities at the time of surgery to drain the normal brain fluid as the brain recovers from the surgery .

Another procedure that is commonly performed, sometimes before a craniotomy, is called a stereotactic biopsy. This smaller operation allows doctors to obtain tissue in order to make an accurate diagnosis. Usually, a frame is attached to the patient's head, a scan is obtained, and then the patient is taken to the operating area, where a small hole is drilled in the skull to allow access to the abnormal area. Based on the location of the lesion, some hospitals may do this same procedure without the use of a frame. A small sample is obtained for examination under the microscope.

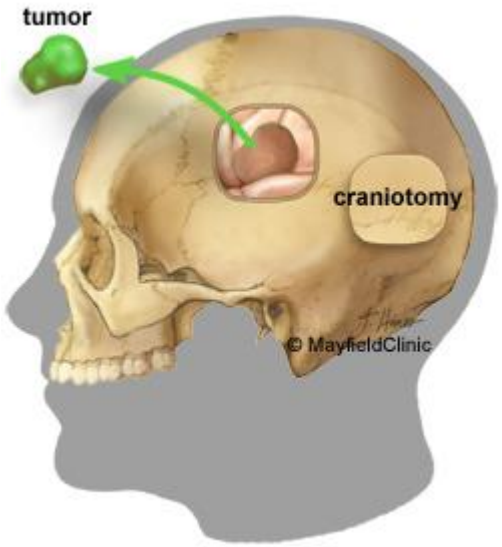

Figure 14. Surgery involves cutting a window in the skull (craniotomy) to remove the tumor.

In the early 1990s, computerized devices called surgical navigation systems were introduced. These systems assisted the neurosurgeon with guidance, localization and orientation for tumors. This information reduced the risks and improved the extent of tumor removal. In many cases, surgical navigation systems allowed previously inoperable tumors to be excised with acceptable risks. Some of these systems also can be used for biopsies without having to attach a frame to the skull. One limitation of these systems is that they utilize a scan (CT or MRI) obtained prior to surgery to guide the neurosurgeon. Thus, they cannot account for movements of the brain that may occur intraoperatively. Investigators are developing techniques using ultrasound and performing surgery in MRI scanners to help update the navigation system data during surgery.

2.2.10.2 Radiation Therapy

Radiation therapy uses high-energy X-rays to kill cancer cells and abnormal brain cells and to shrink tumors. Radiation therapy may be an option if the tumor cannot be treated effectively through surgery.

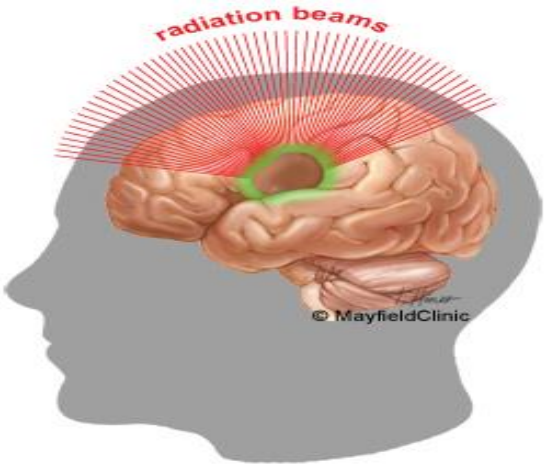

Figure 15. A machine rotates around the patient, aiming radiation beams at the tumor. The radiation beams are shaped to match the tumor and minimize exposure to normal brain tissue.

Standard External Beam Radiotherapy uses a variety of radiation beams to create a conformal coverage of the tumor while limiting the dose to surrounding normal structures. The risk of long-term radiation injury with modern delivery methods is very low. Newer techniques of delivery aside from 3-dimensional conformal radiotherapy (3DCRT) include intensity-modulated radiotherapy (IMRT).

Proton Beam Treatment employs a specific type of radiation in which protons, a form of radioactivity, are directed specifically to the tumor. The advantage is that less tissue surrounding the tumor incurs damage.

Stereotactic Radiosurgery (such as Gamma Knife, Novalis and Cyber knife) is a technique that focuses the radiation with many different beams on the target tissue. This treatment tends to incur less damage to tissues adjacent to the tumor. Currently, there is no data to suggest one delivery system is superior to another in terms of clinical outcome, and each has its advantages and disadvantages.

2.2.10.3 Chemotherapy

Chemotherapy generally is considered to be effective for specific pediatric tumors, lymphomas and some oligodendrogliomas. While it has been proven that chemotherapy improves overall survival in patients with the most malignant primary brain tumors, it does so in only in about 20 percent of all patients, and physicians cannot readily predict which patients will benefit before treatment. As such, some physicians choose not to use chemotherapy because of the potential side effects (lung scarring, suppression of the immune system, nausea, etc…)

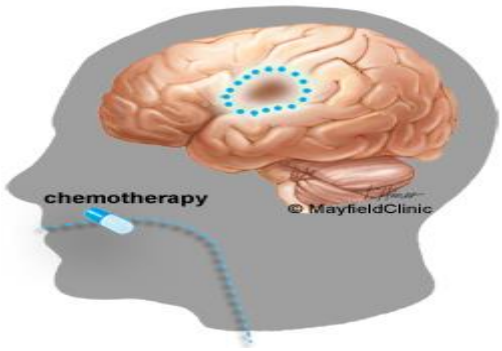

Figure 16. Chemotherapy for high-grade gliomas is usually taken as a pill daily for a set period of time called a cycle. The drug circulates through the bloodstream to the brain where it crosses the blood-brain-barrier to the tumor.

Chemotherapy works by inflicting cell damage that is better repaired by normal tissue than tumor tissue. Resistance to chemotherapy might involve survival of tumor tissue that cannot respond to the drug, or the inability of the drug to pass from the bloodstream into the brain. A special barrier exists between the bloodstream and the brain tissue called the blood-brain barrier. Some investigators have tried to improve the effect of chemotherapy by disrupting this barrier or by injecting the drug into the tumor or brain. The goal of another class of drugs is not to kill the tumor cells but, rather, to block further tumor growth. In some cases, growth modifiers (such as breast cancer treatment drug Tamoxifen) have been used to attempt to stop the growth of tumors resistant to other treatments.

2.2.10.4 Visualase

Laser Thermal Ablation is a newer technique that some centers are using to treat smaller tumors particularly in areas that may be more difficult to reach using previous open surgery procedures. This involves placing a tiny catheter within the lesion, possibly completing a biopsy, then using laser to thermally ablate the lesion. This technique is only more recently used in brain tumor treatments, therefore the long term efficacy has not been established .

2.3 Magnetic Resonance Spectroscopy (MRS)

Magnetic Resonance Spectroscopy (MRS) is an analytical method used in chemistry that enables the identification and quantification of metabolites in samples. It differs from conventional Magnetic Resonance Imaging (MRI) in that spectra provide physiological and chemical information instead of anatomy (Bertholdo et.al 2013).

MRS and MRI have their origin in Nuclear Magnetic Resonance (NMR). NMR was first described in 1946 simultaneously by the Nobel Prize winners Edward Purcell, from Harvard University, and Felix Bloch, from Stanford University. At that time, NMR was used only by physicists for purposes of determining the nuclear magnetic moments of nuclei. It was only in the mid 1970's that NMR started to be used *in vivo*, after Lauterbur, Mansfield and Grannell introduced gradient into the magnetic field enabling them to determinate the location of the emitted signal and to reproduce it in an image. *In vivo* NMR was renamed MRI because the term "nuclear" was constantly and erroneously associated with nuclear medicine. For the same reason, NMR spectroscopy used *in vivo* is now named MRS. During the 1980's, the first MRI medical scanners became available for clinical use. Since then, improvements have been made especially related to higher field strengths (Bertholdo et.al 2013).

MR spectra may be obtained from different nuclei. Protons (^{1}H) are the most used nuclei for clinical applications in the human brain mainly because of its high sensitivity and abundance. The proton MR spectrum is altered in almost all neurological disorders. In some diseases proton MRS (H-MRS) changes are very subtle and not reliable without a statistical comparison between groups of patients. In these cases, H-MRS is usually used for research. In clinical practice, H-MRS is

mostly used for more detailed analysis of primary and secondary brain tumors and metabolic diseases (van der Graaf 2010).

2.3.1 Physical Basis

Many nuclei may be used to obtain MR spectra, including phosphorus (^{31}P), fluorine (^{19}F), carbon (^{13}C) and sodium (^{23}Na). The ones mostly used for clinical MRS are protons (H-MRS). The brain is ideally imaged with H-MRS because of its near lack of motion (this prevents MRS from being used in the abdomen and thorax without very sophisticated motion-reduction techniques). The hydrogen nucleus is abundant in human tissues. H-MRS requires only standard radio-frequency (RF) coils and a dedicated software package. For non-proton MRS, RF coils tuned to the Larmor frequency of other nuclei, matching preamplifiers, hybrids and broad-band power amplifier are needed (Cady and Ernest 2012).

There are different field strengths clinically used for conventional MRI, ranging from 0.2 to 3T. Since the main objective of MRS is to detect weak signals from metabolites, a higher strength field is required (1.5T or more). Higher field strength units have the advantage of higher signal-to-noise ratio (SNR), better resolution and shorter acquisition times making the technique useful in sick patients and others that cannot hold still for long periods of time(Henning and Anke. 2008).

H-MRS is based on the chemical shift properties of the atom. When a tissue is exposed to an external magnetic field, its nuclei will resonate at a frequency (*f*) that is given by the Larmor equation:

$$f = \gamma B0$$

Since the gyromagnetic ratio (γ) is a constant of each nuclear species, the spin frequency of a certain nuclei (*f)* depends on the external magnetic field (*B*0) and the local microenvironment. The electric shell interactions of these nuclei with the

surrounding molecules cause a change in the local magnetic field leading to a change on the spin frequency of the atom (a phenomenon called chemical shift). The value of this difference in resonance frequency gives information about the molecular group carrying ^{1}H and is expressed in parts per million (ppm). The chemical shift position of a nucleus is ideally expressed in ppm because it is independent of the field strength (choline, for example, will be positioned at 3.22 ppm at 1.5T or 7T). The MR spectrum is represented by the x axis that corresponds to the metabolite frequency in ppm according to the chemical shift and the y axis that corresponds to the peak amplitude (Fig. 17).

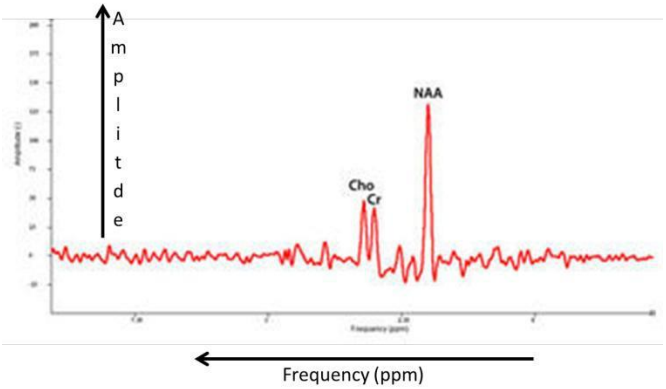

Fig. 17. Normal spectra. y axis correspond to amplitude and x axis to the metabolites frequency

Some metabolites such as lactate have doublets, triplets or multiplets instead of single peaks. These peaks are broken down into more complex peaks and are explained by J-coupling, also named spin-spin coupling. The j-coupling phenomenon occurs when the molecular structure of a metabolite is such that protons are found in different atomic groups (for example CH3- and –CH2-). These groups have a slightly different local magnetic fields, thus each ^{1}H resonates at a frequency characteristic of its position in the molecule resulting in a multiplet peak (Grover et al 2015).

2.3.2 Techniques

The H-MRS acquisition usually starts with anatomical images, which are used to select a volume of interest (VOI), where the spectrum will be acquired. For the spectrum acquisition, different techniques may be used including single- and multi-voxel imaging using both long and short echo times (TE). Each technique has advantages and disadvantages and choosing the right one for a specific purpose is important to improve the quality of the results (Bertholdo et.al 2013).

2.3.2.1 Single-Voxel Spectroscopy

In the single voxel spectroscopy (SVS) the signal is obtained from a voxel previously selected. This voxel is acquired from a combination of slice-selective excitations in three dimensions in space, achieved when a RF pulse is applied while a field gradient is switched on. It results in three orthogonal planes and their intersection corresponds to VOI (Fig. 18).

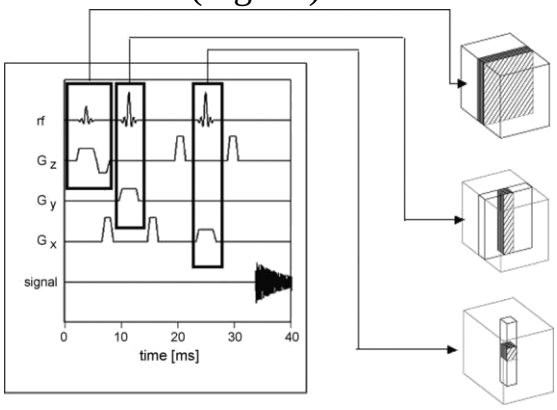

Fig. 18. SVS. The intersection of the orthogonal planes, given by slice selection and phase gradients, results in the VOI.

Mainly, two techniques are used for acquisition of SVS H-MRS spectra: pointed-resolved spectroscopy (PRESS) and stimulated echo acquisition mode (STEAM).

The most used SVS technique is PRESS. In the PRESS sequence, the spectrum is acquired using one 90^{o} pulse followed by two 180^{o} pulses. Each of them is applied

at the same time as a different field gradient. Thus, the signal emitted by the VOI is a spin echo. The first 180º pulse is applied after a time TE1/2 from the first pulse (90º pulse) and the second 180º is applied after a time TE1/2+TE. The signal occurs after a time 2TE (Fig. 19). To restrict the acquired sign to the VOI selected, spoiler gradients are needed. Spoiler gradients dephase the nuclei outside the VOI and reduce their signal.

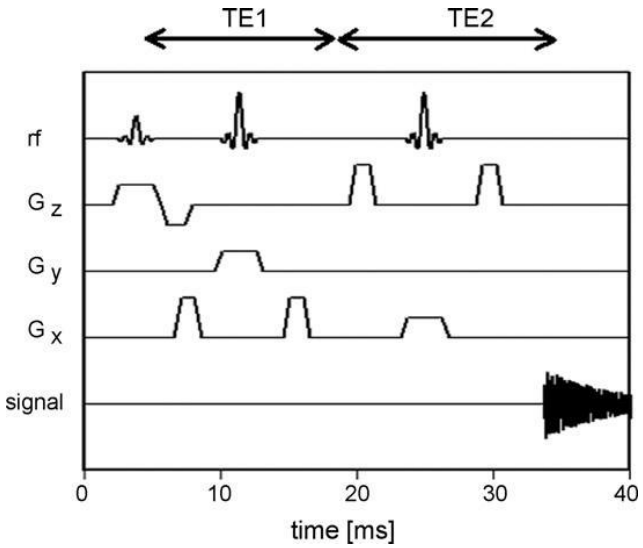

Fig. 19. PRESS

STEAM is the second most commonly used SVS technique. In this sequence all three pulses applied are 90º pulses. As in PRESS, they are all simultaneous with a different field gradients. After a time TE1/2 from the first pulse, a second 90º is applied. The time elapsed between the second and the third is conventionally called "mixing time" (MT) and is shorter than TE1/2. The signal is finally achieved after a time TE+MT from the first pulse (Fig. 20). Thus, the total time for STEAM technique is shorter than PRESS. Spoiler gradients are also needed to reduce signal from regions outside the VOI.

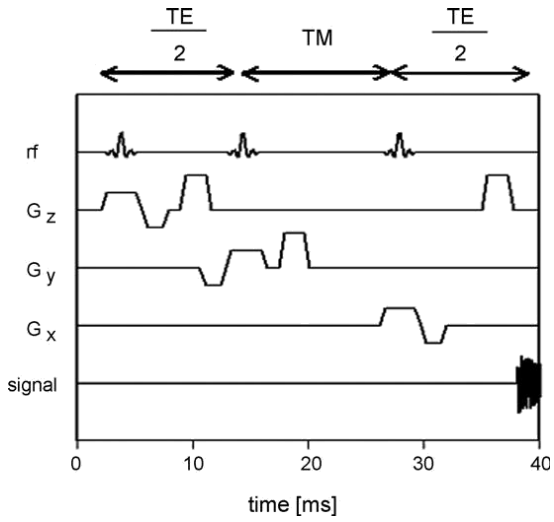

Fig. 20 STEAM

Because STEAM sequence uses only 90^{o} pulses, it has 50% lower SNR than PRESS. As stated before, PRESS sequence is acquired using two pulses of 180^{o}. The use of these 180^{o} pulses results in a less optimal VOI profile and leads to higher SNR. However, since the length of 180^{o} pulses is longer than 90^{o}, PRESS cannot be achieved with a very short TE. Another disadvantage of PRESS sequence is the larger chemical shift displacement artifact, which is described later in this chapter.

Therefore, STEAM is usually the modality of choice when a short TE and precise volume selection is needed. On the other hand, PRESS is the mostly used SVS technique because it doubles SNR, which is an important factor leading to better spectral quality(Bertholdo et.al 2013).

2.3.2.2 Magnetic Resonance Spectroscopy Imaging (MRSI)

Magnetic resonance spectroscopy imaging (MRSI), also called spectroscopic imaging or chemical shift imaging, is a multi-voxel technique. The main objective of MRSI is to obtain simultaneously many voxels and a spatial distribution of the metabolites within a single sequence. Thus, this H-MRS technique uses phase-

encoding gradients to encode spatial information after the RF pulses and the gradient of slice selection (Mandal et.al 2012).

MRSI is acquired using only slice selection and phase encoding gradients, besides the spoiler gradients. Differently from conventional MRI, a frequency encoding gradient is not applied in MRSI (FIGURE 5). Thus, instead of the anatomical information given by the conventional MRI signal, the MRS signal results in a spectrum of metabolites with different frequencies (information acquired from chemical shift properties of each metabolite).

The same sequences used for SVS are used for the signal acquisition in MRSI (STEAM or PRESS). The main difference between MRSI and SVS is that, after the RF pulse, phase encoding gradients are used in one, two or three dimensions (1D, 2D or 3D) to sample the *k*-space (Fig. 21). In a 1D sequence, the phase encoding has a single direction, in 2D has two orthogonal directions and, in 3D three orthogonal directions.

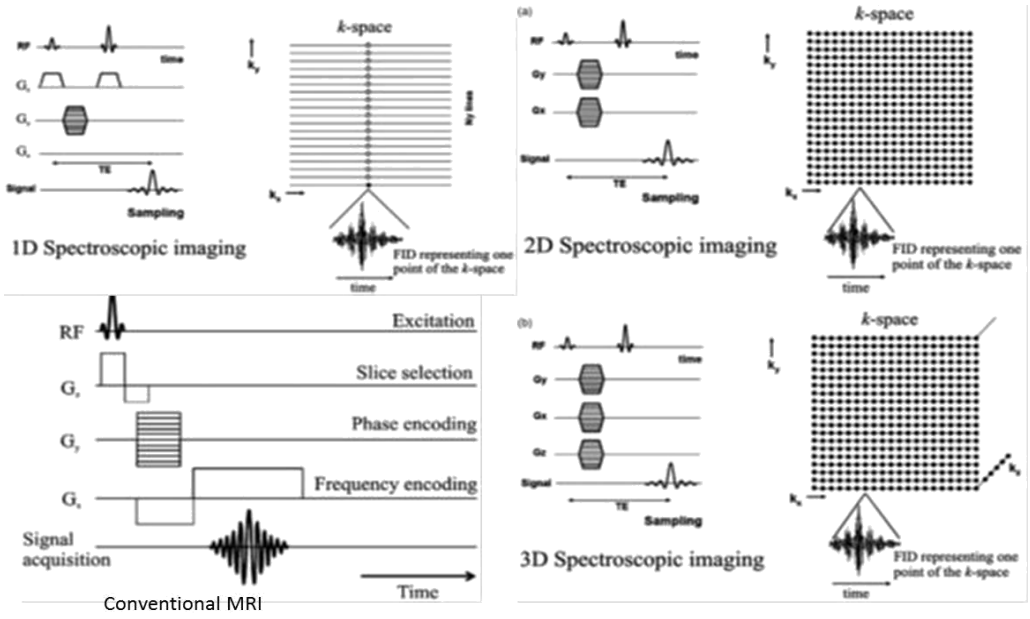

Fig. 21. 1D MRSI (a); 2D MRSI (b); 3D MRSI (c) and conventional MRI (d)

The result of a 2D MRSI is a matrix, called a spectroscopy grid. The size of this grid corresponds to the field of view (FOV) previously determined. In the 3D sequence, many grids are acquired within one FOV. The number of partitions (or voxels) of the grids is directly proportional to the number of phase encoding steps. The spatial resolution is also proportional to the number of voxels in a determined FOV (more voxels give a better spatial resolution). However, for a larger number of voxels, more phase encoding steps are needed and this implies a longer time for acquisition. Spatial resolution is also determined by the FOV size (smaller FOV gives better spatial resolution) and by *point of spread function* (PSF).

PSF on an optical system is defined as the distribution of light from a single point source. For MRSI the PSF is related to voxel contamination with signals from adjacent voxels, also called voxel "bleeding". This same effect corresponds to the Gibbs ringing artifact seen on conventional MRI. The shape of PSF is determined by the *k*-space sampling method and the number of phase encoding steps. PSF can be avoided when more than 64-phase encoding steps are applied, which leads to a time of scanning not feasible in clinical practice. To reduce PSF some methods are used such as *k*-space filtering and reduction. For *k*-space reduction, the data only inside a circular (2D) or spherical (3D) region are measured (Fig. 22).

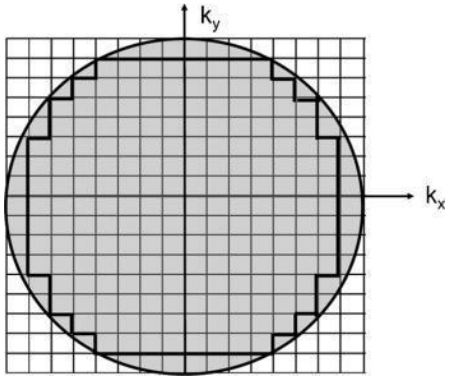

Fig. 22. Circular 2D k-space sampling. Only the data inside the area of k-space delimited by the circle is measured. The remaining space is filled with zero.

Another concern about MRSI is the suppression of unwanted signals from outside of the brain, particularly from the subcutaneous fat, since lipids have a much higher signal than brain metabolites. Since an FOV has always a rectangular

shape and the brain is oval shaped, some techniques must be used to optimize the FOV. The use of outer-volume suppression (OVS) as shown on the (figure . 23) is the most used technique for this purpose.

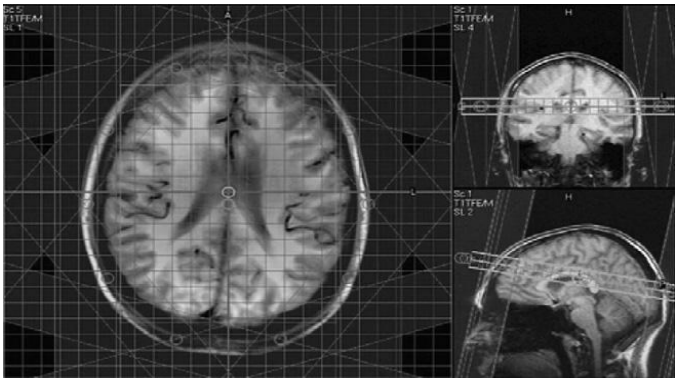

Fig. 23. Use of OVS to minimize unwanted signal from outside the brain

All techniques that help optimize the MRSI sequence by reducing voxel bleeding and increasing spatial resolution and the number of phase encoding needed to acquire a 2D or 3D MRSI have a cost: time. Therefore, in order to minimize scan time without reducing quality, fast MRSI techniques are used. First, it is important to know that, FOV has a significant role on scanning time. A large FOV means a longer the time to acquire the MRSI spectrum. A simple way to reduce time is to use the smallest FOV possible consistent with the dimension of the object to be analyzed.

Reducing the *k*-space sampling by measuring the data inside a circular or spherical region instead of a rectangular one is another way to reduce scan time (Fig. 6). Other techniques used for this purpose are turbo-MRSI (using multiple spin-echos), multi-slice MRSI, three-dimensional echo-planar spectroscopic imaging (EPSI), and parallel imaging methods. These techniques are beyond the scope of

this chapter and for more details can be found elsewhere (Duyn and Moonen, 1993; Duyn et al., 1993; Posse et al., 1994).

2.3.2.3 SVS vs MRSI

SVS and MRSI have advantages and disadvantages regarding their use for specific purposes (Table 1) SVS technique results in a high quality spectrum, a short scan time, and good field homogeneity. Thus, SVS technique is usually obtained with short TE since longer TE has decreased signal due to T2 relaxation. SVS is used to obtain an accurate quantification of the metabolites(Bertholdo et.al 2013).

The main advantage of MRSI is spatial distribution compared to SVS technique that only acquires the spectrum in a limited brain region. Moreover, the grid obtained with MRSI allows voxels to be repositioned during post processing. On the other hand, the quantification of the metabolites is not as precise when using MRSI technique because of voxel bleeding. Therefore, MRSI can be used to determinate spatial heterogeneity.

Table 3: Difference between single voxel spectroscopy (SVS) and magnetic resonance spectroscopy imaging (MRSI)

SVS	**MRSI**
Short TE	Long TE
One voxel	Multi-voxel
Limited region	Many data collected
Fixed grid	Grid may be shifted after acquisition
More accurate	Voxel bleeding
Quantitative measurement	Spatial distribution

2.3.2.4 Short TE vs long TE

MRS can be obtained using different TEs that result in distinct spectra. Short TE refers to a study in which it varies from 20 to 40 ms. It has a higher SNR and less signal loss due to T2 and T1 weighting than long TE. These short TE properties result in a spectrum with more metabolites peaks, such as myoinositol and glutamine-glutamate (Fig. 8), which are not detected with long TE. Nevertheless, since more peaks are shown on the spectrum, overlap is much more common and care must be taken when quantifying the peaks of metabolites (Bertholdo et.al 2013).

MRS spectra may also be obtained with long TEs, from 135 to 288 ms. Some authors describe 135-144 ms as an intermediate TE, but in this chapter we will include it along with long TEs. Long TEs have a worse SNR, however they have a more simple spectra due to suppression of some signals. Thus, the spectra are less noisy but have a limited number of sharp resonances. On 135-144 TEs the peak of lactate is inverted below the baseline. This has an important value since the peaks of lactate and lipids overlap in this spectrum. Therefore, 135-144 TEs allow for easier recognition of lactate peak (Fig. 24) as lipids remain above the baseline. With TE of 270-288 ms there is a lower SNR and the lactate peak is not inverted.

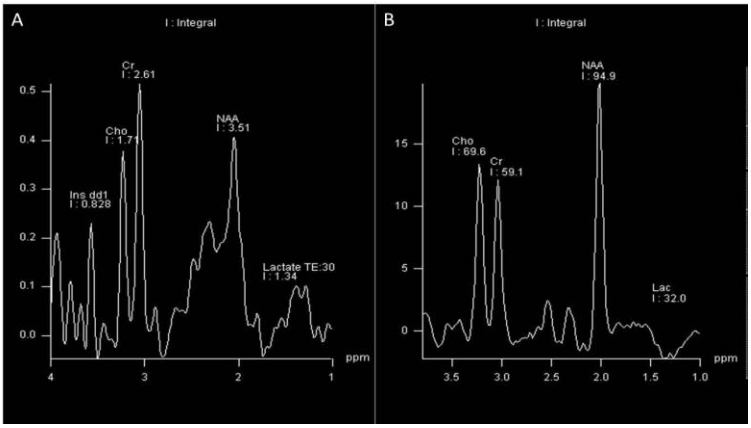

Fig. 24. Spectrum obtained with TE = 30ms (A) and TE = 135ms (B). Note the inverted lactate peak (doublet) with long TE acquisition and the more number of sharps resonance with short TE. Cho– choline; Cr- creatine NAA– N-acetylaspartate; Ins dd1– myoinositol.

2.3.3 Water Suppression

MRS-visible brain metabolites have a low concentration in brain tissues. Water is the most abundant and thus its signal in MRS spectrum is much higher than that of other metabolites (the signal of water is 100.000 times greater than that of other metabolites). To avoid this high peak from water to be superimpose on the signal of other brain metabolites, water suppression techniques are needed (fig. 25). The most commonly used technique is chemical shift selective water suppression (CHESS) which pre-saturates water signal using frequency selective 90º pulses before the localizing pulse sequence. Other techniques sometimes used are VAriable Pulse power and Optimized Relaxation Delays (VAPOR) and Water suppression Enhanced Through T1 effects (WET).

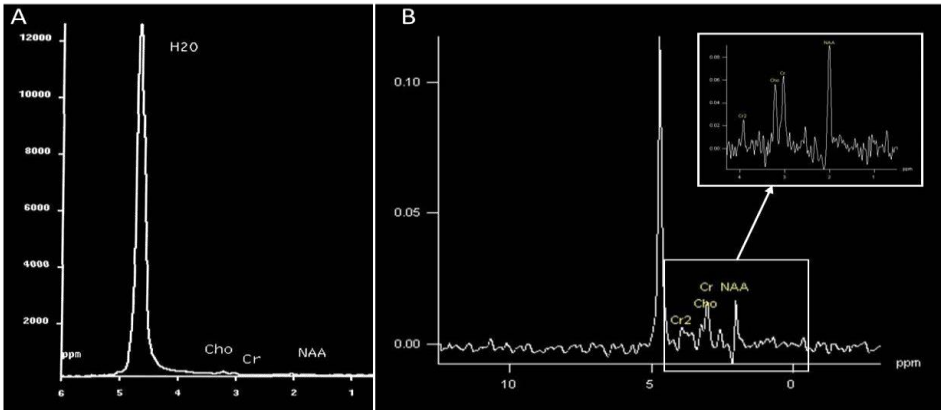

Fig. 25. Water signal suppressing with CHESS. Spectrum before CHESS (A) and after CHESS (B). CHESS reduces signal from water by a factor of 1000 allowing brain metabolites to be depicted on the spectrum.

2.3.4 Post-processing

Quantification and analysis methods of collected data are as important as the acquisition techniques use to obtain the spectra. Using an incorrect post-processing

method may lead to wrong interpretations. There are many post-processing techniques that may be used before and after the Fourier transform (FT).

The properties of the spectrum may be manipulated using digital filters before the FT. Zero-filling, multiplication with a filter, eddy-current correction, and band-reject filters are some examples of post-processing steps during time domain. The use of zero-filling results in a higher digital resolution in the spectrum. Band-reject filters are used to remove residual water signal when water suppression technique used during signal acquisition did not completely eliminate it. Eddy-current correction is used to eliminate eddy-current artifacts (explained in the artifact section) using a reference signal such as unsuppressed water signal and applying a time-dependent phase correction. After the FT, during frequency domain, phase and base line correction are usually used. All these post-processing methods may be used with SVS and MRSI. However, since MRSI uses phase-encoding gradients, other filters need to be applied before FT (e.g. "Haning"or Hamming filters" and "Fermi"filter) (Bertholdo et.al 2013).

2.3.5 Artifacts

MRS is prone to artifacts. Motion, poor water or lipid suppressions, field inhomogeneity, eddy currents, and chemical shift displacement are some examples of factors that introduce artifacts into spectra. One of the most important factors that predict the quality of a spectrum is the homogeneity of the magnetic field. Poor field homogeneity results in a lower SNR and broadening of the width of the peaks. For brain MRS, some regions are more susceptible to this artifact, including those near bone structures and air tissue- interfaces. Therefore placement of the VOI should be avoided near areas such as anterior temporal and frontal lobes. Paramagnetic devices also result in field heterogeneity leading to a poor quality spectrum when the VOI is placed near them (Bertholdo et.al 2013).

Eddy currents are caused by gradient switching. A transient current results in distortion of the peak shapes, making spectrum quantification difficult. This artifact is more commonly seen in older MRI units. However, even modern units produce smaller eddy current artifacts and eddy current correction (used on post-procession phase) is needed.

Chemical shift displacements correspond to chemical shift artifacts on conventional MRI. The localization of the voxel is based on the precession frequency of the protons. Since this frequency is different for each metabolite, the exact position of each metabolite is slightly different. This artifact is larger with higher magnetic field strengths. To solve this problem, strong field gradients for the slice selection must be used(Barker P B et.al 2010).

2.3.6 Higher Fields H-MRS

Higher field MRI (3T, 7T and above) is used in many centers mostly for research purposes. On the past decade, 3T MRI started to be routinely used for clinical examinations and it results in better SNR and faster acquisitions factor which are important in sick patients that cannot hold still.

H-MRS performed at 3T MRI has a higher SNR and a reduced acquisition time compared to 1.5T. It was believed that SNR would increase linearly with the strength of the magnetic field but SNR does not double with 3T H-MRS because others factors are also responsible for the SNR, including metabolite relaxation time and magnetic field homogeneity.

Spectral resolution is improved with higher magnetic field. A better spatial resolution increases the distance between peaks making it easier to distinguish between them. This is important particularly for resonances from coupled spins such as glutamate, glutamine and myo-inositol. However, the metabolites

linewidth also increases at higher magnetic field due to a markedly increase T2 relaxation time. Thus, short TE is more commonly used with 3T. The difference of T1 relaxation time from 1.5T to3T depends on the brain region studied (Ethofer, 2003).

3T H-MRS is more sensitive to magnetic field inhomogeneity andsome artifacts are more pronounced with it particularly susceptibility and eddy currents ones. Chemical shift displacement is also larger at 3T and this artifact increases linearly with the magnetic field.Not only field strength has improved on the past few years, but also receiver coils. The use of multiple radiofrequency receiver coils for MRS provides higher local sensitivity and results in higher SNR. These coils also allow a more extended coverage of the brain(Lacey et al.1999).

2.3.7 Spectra

H-MRS allows the detection of brain metabolites. The metabolite changes often precede structural abnormalities and MRS can demonstrate abnormalities before MRI does (Fayed et al., 2006). To detect these spectral alterations, it is fundamental to know the normal brain spectra and their variations according to the each technique, patient age, and brain region.^{1}H spectra of metabolites are shown on x and y axes. The x, horizontal, axis displays the chemical shift of the metabolites in units of ppm. The ppm increases from right to left. The y, vertical, axis demonstrates arbitrary signal amplitude of the metabolites. The height of metabolic peak refers to a relative concentration and the area under the curve to metabolite concentration (Fayed et al., 2006).

Long TE sequences result in less noise than short TE sequences but several metabolites are better demonstrated with short TE. In 1.5T MR scanners, long TE sequences (TE = 135-288 ms) detect NAA, Cr, Cho, Lac and possibly Ala. Short TE sequences (TE = 20-40 ms) demonstrate the metabolites seen with long TE

acquisitions and in addition Lip, Myo, Glx, glucose, and some macromolecular proteins) (Fig. 26).

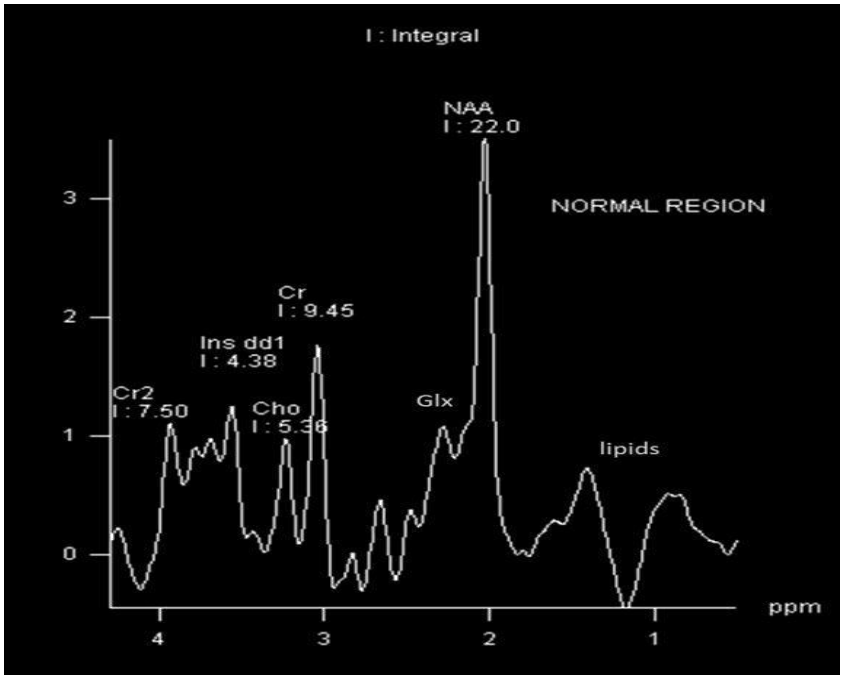

Fig. 26. Normal spectra obtained with short TE sequence. (TE= 30ms). Ins dd1– myoinositol; Cho– choline; Cr- creatine; Glx-glutamate-glutamine; NAA– n-acetylaspartate.

2.3.8 Brain metabolites

2.3.8.1 N-acetylaspartate (NAA)

Peak of NAA is the highest peak in normal brain. This peak is assigned at 2.02 ppm. NAA is synthesized in the mitochondria of neurons then transported into neuronal cytoplasm and along axons. NAA is exclusively found in the nervous system (peripheral and central) and is detected in both grey and white matter. It is a marker of neuronal and axonal viability and density. NAA can be found in immature oligodendrocytes and astrocyte progenitor cells, as well. NAA also plays a role as a cerebral osmolyte.

Absence or decreased concentration of NAA is a sign of neuronal loss or degradation. Neuronal destruction from malignant neoplasms and many white matter diseases result in decreased concentration of NAA. In contrast, increased NAA is nearly specific for Canavan disease. NAA is not demonstrated in extra-axial lesions such as meningiomas or intra-axial ones originating from outside of the brain such as metastases(Soares and Law, 2009).

2.3.8.2 Creatine (Cr)

The peak of Cr spectrum is assigned at 3.02 ppm. This peak represents a combination of molecules containing creatine and phosphocreatine. Cr is a marker of energetic systems and intracellular metabolism. Concentration of Cr is relatively constant and it is considered a most stable cerebral metabolite. Therefore it is used as an internal reference for calculating metabolite ratios. However, there are regional and individual variability in Cr concentrations. In brain tumors, there is a reduced Cr signal (see details below). On the other hand, gliosis may cause minimally increased Cr due to increased density of glial cells (glial proliferation). Creatine and phosphocreatine are metabolized to creatinine then the creatinine is excreted via kidneys (Hajek and Dezortova, 2008). Systemic disease (e.g. renal disease) may also affect Cr levels in the brain (Soares and Law, 2009).

2.3.8.3 Choline (Cho)

Its peak is assigned at 3.22 ppm and represents the sum of choline and choline-containing compounds (e.g. phosphocholine). Cho is a marker of cellular membrane turnover (phospholipids synthesis and degradation) reflecting cellular proliferation. In tumors, Cho levels correlate with degree of malignancy reflecting of cellularity. Increase Cho may be seen in infarction (from gliosis or ischemic damage to myelin) or inflammation (glial proliferation) hence elevated Cho is nonspecific (Soares and Law, 2009).

2.3.8.4 Lactate (Lac)

Peak of Lac is not seen or is hardly visualized in the normal brain. The peak of Lac is a doublet at 1.33 ppm which projects above the baseline on short/long TE acquisition and inverts below the baseline at TE of 135-144 msec.

A small peak of Lac can be visible in some physiological states such as newborn brains during the first hours of life (Mullins, 2006). Lac is a product of anaerobic glycolysis so its concentration increases under anaerobic metabolism such as cerebral hypoxia, ischemia, seizures and metabolic disorders (especially mitochondrial ones). Increased Lac signals also occur with macrophage accumulation (e.g. acute inflammation). Lac also accumulates in tissues with poor washout such as cysts, normal pressure hydrocephalus, and necrotic and cystic tumors (Soares and Law, 2009).

2.3.8.5 Lipids (Lip)

Lipids are components of cell membranes not visualized on long TE because of their very short relaxation time. There are two peaks of lipids: methylene protons at 1.3 ppm and methyl protons at 0.9 ppm (van der Graaf, 2010). These peaks are absent in the normal brain, but presence of lipids may result from improper voxel selection causing voxel contamination from adjacent fatty tissues (e.g. fat in subcutaneous tissue, scalp and diploic space).

Lipid peak scan be seen when there is cellular membrane breakdown or necrosis such as in metastases or primary malignant tumors(Soares and Law, 2009).

2.3.8.6 Myoinositol (Myo)

Myo is a simple sugar assigned at 3.56 ppm. Myo is considered a glial marker because it is primarily synthesized in glial cells, almost only in astrocytes. It is also the most important osmolyte in astrocytes. Myo may represent a product of myelin

degradation. Elevated Myo occurs with proliferation of glial cells or with increased glial-cell size as found in inflammation. Myo is elevated in gliosis, astrocytosis and in Alzheimer's disease (Soares and Law, 2009; van der Graaf, 2010).

2.3.8.7 Alanine (Ala)

Ala is an amino acid that has a doublet centered at 1.48 ppm. This peak is located above the baseline in spectra obtained with short/long TE and inverts below the baseline on acquisition using TE= 135-144 msec . Its peak may be obscured by Lac (at 1.33 ppm). The function of Ala is uncertain but it plays a role in the citric acid cycle (Soares & Law, 2009). Increased concentration of Ala may occur in oxidative metabolism defects (van der Graaf, 2010). In tumors, elevated level of Ala is specific for meningiomas (Soares and Law, 2009).

2.3.8.8 Glutamate-Glutamine (Glx)

Glx is a complex peaks from glutamate (Glu), Glutamine (Gln) and gamma-aminobutyric acid (GABA) assigned at 2.05-2.50 ppm. These metabolite peaks are difficult to separate at 1.5 T. Glu is an important excitatory neurotransmitter and also plays a role in the redox cycle (Soares and Law, 2009; van der Graaf, 2010). Elevated concentration of Gln is found in a few diseases such as hepatic encephalopathy (Fayed et al., 2006; van der Graaf, 2010).

2.3.9 Regional variations of the spectra

Metabolite peaks may slightly differ according to the brain region studied. Studies have shown differences between the spectra of white and gray matter and supratentorial and infratentorial structures. Nevertheless, no significant asymmetries of metabolite spectra between the left and the right hemispheres nor between genders have been found (Charles et al., 1994; Nagae-Poetscher et al., 2004).

In specific quantitative techniques, concentration of NAA in grey matter is higher than that in white matter. For clinical purposes concentrations of NAA in both grey and white matter are not significantly different. Most studies have found higher Cho levels in white matter than in grey matter whereas Cr level is higher in grey matter (Hajek and Dezortova, 2008; Hetherington et al., 1994; Kreis et al., 1993a; Soher et al., 1996). There are some frontal-occipital variations too. The most outstanding difference is a caudally decreased in Cho in the cortex (Degaonkar et al., 2005; Pouwels and Frahm, 1998). Regional variations of Glx and Myo have been studied less than those of NAA, Cho and Cr. One study (Baker et al., 2008) found higher Glx levels in grey matter than in white matter. The regional distribution of Myo is unclear but tends to be higher in grey than in white matter

Of the brainstem and cerebellum the highest levels of NAA are in the pons (Jacobs et al., 2001). Significantly higher levels of Cho have been found in the cerebellum and pons compared to supratentorial regions (Jacobs et al., 2001; Pouwels and Frahm, 1998). Cerebellar levels of Cr are also significantly higher than supratentorial levels while low levels of Cr are seen in the pons (Jacobs et al., 2001; Pouwels and Frahm, 1998).MRS of the hippocampus has been studied especially in epilepsy and Alzheimer disease. There are anterior-posterior gradients of metabolites in the hippocampi. Concentration of Cho increases from posterior to anterior hippocampus whereas lower NAA has been found anteriorly (Arslanoglu et al., 2004; Vermathen et al., 2000).

2.3.10 Spectra in pediatrics

Regardless of the differences in methodology, there are differences in metabolite levels in the developing brain. MR spectra depend on age and during the first year of life significant changes occur. In general, the spectral pattern in pediatrics is considered to be similar to that of the adults older than 2 years of age and the

concentration of metabolites is practically constant by 4 years of age (Dezortova & Hajek, 2008; Kreis et al., 1993b; Soares & Law, 2009). NAA levels are low whereas Myo and Cho levels are high at birth. Both grey and white matter show similar patterns. Myo is a prominent metabolite in brain spectra of newborns. As age increases, increased concentration of NAA and decreased concentrations of choline-containing compounds and Myo become evident (Dezortova & Hajek, 2008; Fayed et al., 2006; Soares and Law, 2009). Concentrations of creatine and phosphocreatine are constant and may be used as reference values (Fig 27). Increased concentration of NAA reflects brain maturation and its concentration correlates with myelination (Dezortova and Hajek, 2008; Hajek and Dezortova, 2008). With cerebral maturation, there is also a decrease in concentration of choline compounds. A small amount of Lac may be seen in newborn brains (Mullins, 2006). Glu and Gln do not demonstrate significant alterations with age (Dezortova & Hajek, 2008).

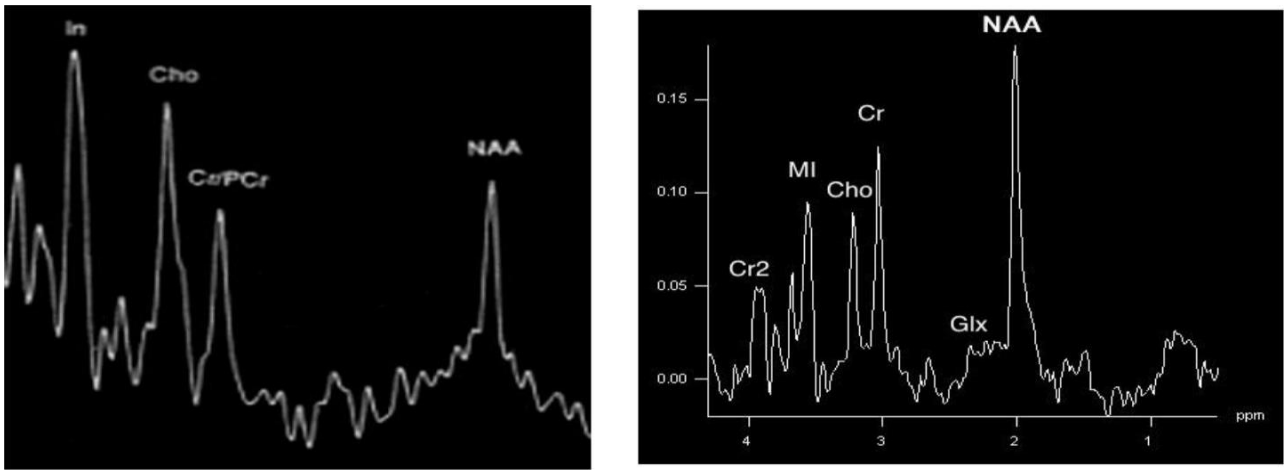

Fig. 27. Normal spectra in newborn (left) and adult (right).Remarks:

In and MI represent Myo.

According to gestational age, the equation of Kreis et al. (Kreis et al., 1993b) describes metabolite concentration changes. With this equation and parameters for a multiexponential model (Dezortova & Hajek, 2008) graphs of metabolite changes with age can be drawn (Fig. 28).

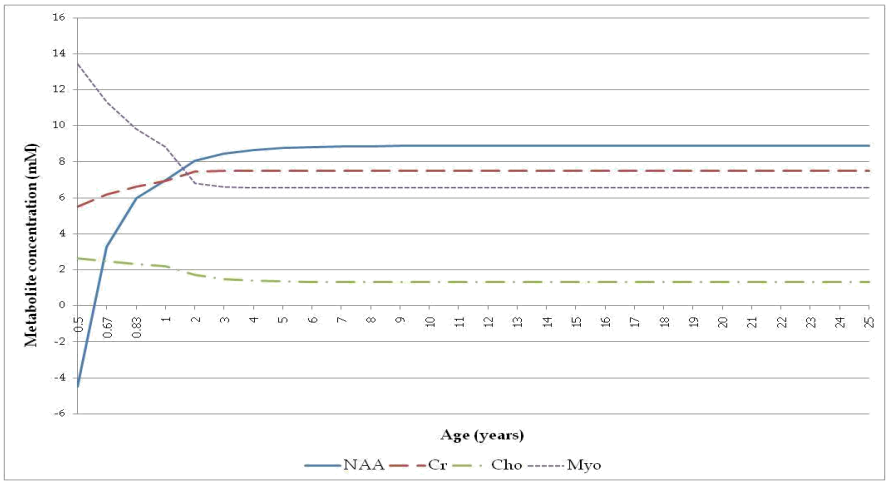

Fig. 28. Changes in metabolite concentrations with age calculated by the equation of Kries et al. and the parameters of Dezortova and Hajek.

2.3.11 Spectra in elderly

MRS studies of elderly brains are less consistent than those of pediatric brains. Some studies have found reduced concentration of NAA with aging which suggests a decrease in neuronal mass (Christiansen et al., 1993; Lim and Spielman, 1997; Soares and Law, 2009). In contrast, the other studies have found relatively stable concentrations of NAA in older groups, but increased Cho and/or Cr (Chang et al., 1996; Soher et al., 1996). A systematic review of MRS in healthy aging summarized the findings of MRS in aging in that they are varied. Most studies have reported no changes in metabolites with advanced age. However, some data suggest lower NAA and higher Cho and Cr with increasing age (Haga et al., 2009). Disagreement of the studies could be due to the use of different techniques (e.g.

different evaluated brain regions and atrophy correction) Different study populations may also affect results.

2.3.12. Clinical Application

2.3.12.1 Brain Tumors

Brain tumors are currently the main application of H-MRS. This technique is usually used as a complement to conventional MRI, along with other advanced techniques, such as perfusion. Combined with conventional MRI, proton MR spectra may improve diagnosis and treatment of brain tumors. H-MRS may help with differential diagnosis, histologic grading, degree of infiltration, tumor recurrence, and response to treatment mainly when radionecrosis develops and is indistinguishable from tumor by conventional MRI.

An important decision regarding analysis of intracranial masses is which H-MRS technique to use. Different H-MRS parameters may be varied to optimize the results. The most relevant parameter when facing is TE (Majós et al., 2004). Short TE allows for recognition of more peaks than long TE, which may be important for differential diagnosis of brain masses and for grading tumors. Myo is a marker for low grade gliomas, only seen on short TE acquisitions. On the other hand, longer TEs give a spectrum with a limited number of peaks making it easier to analyze. Long TEs varying from 135-140ms also invert peaks of Lac and Ala. This inversion is important for differentiating between these peaks and lipids since they commonly overlap. Hence, the choice of TE may be difficult and one solution is to acquire two different spectra using both TEs. In clinical practice two H-MRS acquisitions are rarely feasible due to time constraints.

MRSI is usually preferable to SVS because of its spatial distribution. It allows the acquisition of a spectrum of a lesion and the adjacent tissues and also gives a better

depiction of tumor heterogeneity. However, MRSI is generally combined with long TE instead of short TE. SVS, on the other hand, is faster and can be obtained using both long and short TEs. When using SVS, the VOI should be placed within the mass, avoiding contamination from adjacent tissues. An identical VOI must be positioned on the homologous region of the contralateral hemisphere for comparison, whenever possible (Gupta et al., 2000).

Elevation of Cho is seen in all neoplastic lesions. Cho peak may help with treatment response, diagnosis and progression of tumor. Its increase has been attributed to cellular membrane turnover which reflects cellular proliferation. One prospective study (Gupta et al., 2000) analyzing 18 gliomas showed that Cho signal was linearly correlated with cell density (inversely to what is seen with apparent diffusion coefficient) instead of proliferative index. Cho peak is usually higher in the center of a solid neoplastic mass and decreases peripherally. Cho signal is consistently low in necrotic areas.

Another H-MRS feature seen in brain tumors is decrease NAA. This metabolite is a neuronal marker and its reduction denotes destruction and displacement of normal tissue. Absence of NAA in an intra-axial tumor generally implies an origin outside of the central nervous system (metastasis) or a highly malignant tumor that has destroyed all neurons in that location. Cr signal, on the other hand, is slightly variable in brain tumors. It changes according to tumor type and grade. The typical H-MRS spectrum for a brain tumor is one of high level of Cho, low NAA and minor changes in Cr (Fig. 29) (Majós et al., 2004)..

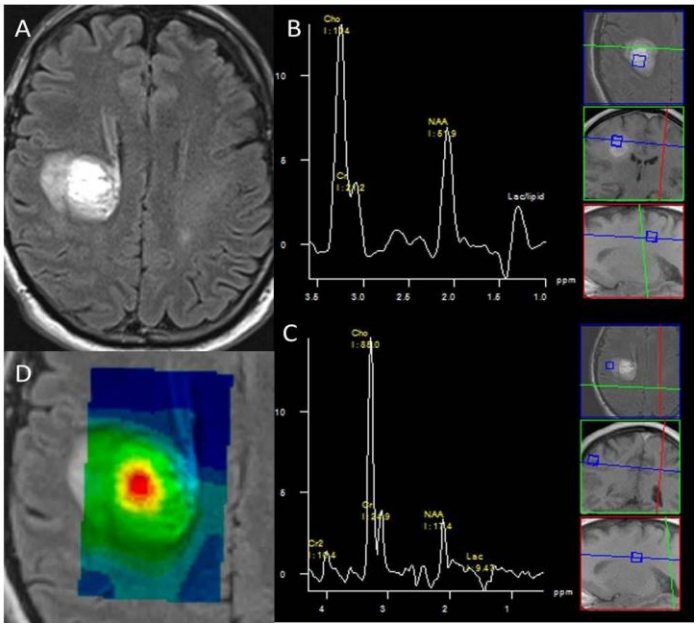

Fig. 29. Histologically confirmed glioblastoma. Axial FLAIR MR images (A) show an expansive lesion with high signal intensity on the right frontal lobe. H-MRS with long TE demonstrates increase in Cho peak and decrease in NAA peak inside the lesion (B) and in the surrounding abnormal tissue (C) representing tumor infiltration. Lactate and lipids are also present. Color metabolite map (D) also demonstrate abnormal Cho/Cr ratio.

Cho elevation is usually evidenced by increase in Cho/NAA or Cho/Cr ratios, rather than its absolute concentration. Estimation of absolute Cho concentration, although possible, is susceptible to many errors since many assumptions are required. Therefore, Cho/NAA and Cho/Cr ratios are accurate for establishing Cho levels in brain neoplasms.

When faced with intracranial expansive lesions, conventional MRI with or without perfusion may lead to a reliable diagnosis. In doubtful cases, H-MRS may play a role in pre-operative differential diagnosis (table 2). Studies have shown that the use of H-MRS in specific cases improves accuracy and level of confidence in differentiating neoplastic from non-neoplastic masses (Majós et al., 2009). The differentiation of a low grade glioma (LGG) from stroke or focal cortical dysplasia

(fig. 30) may be difficult or impossible using conventional MRI. In these cases, increased levels of Cho make diagnosis of neoplasm much more likely. In some cases of focal cortical dysplasia, Cho may be moderately increased probably as a result of intrinsic epileptic ictal activity (Vuor et al., 2004).

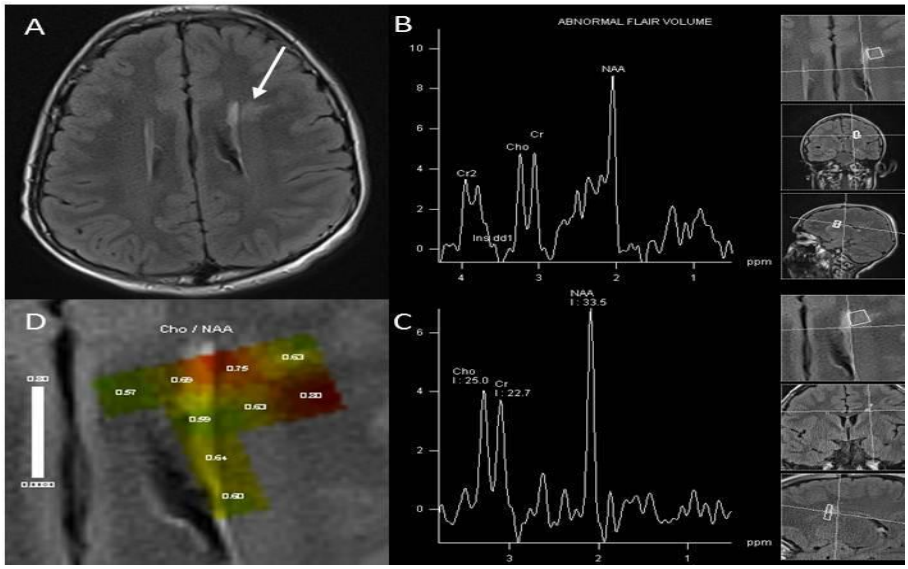

Fig.30. Ten year-old boy with intractable seizures. (A) FLAIR image show a focal high signal intensity in the white matter of the centrum semiovale of the left frontal lobe(white arrow). H-MRS with TE= 35ms (B) and TE=144 (C) demonstrate normal Cho and NAA peaks. Color metabolite map (D) demonstrate normal Cho/NAA ratio. These findings are suggestive of a cortical dysplasia with adjacent abnormal white matter.

Some expansible lesions may be similar to neoplasms on conventional MRI and H-MRS. H-MRS spectrum of a giant demyelinating plaque usually shows high Cho and low NAA levels. In the acute stage of a demyelinating disease, increase Lac can also be seen and may reflect the metabolism of inflammatory cells (De Stefano et al., 2007; Bitsch et al., 1999). Increase in glutamate (Srinivasan et al., 2005) and Myo (Fernando et al., 2004) is also noted in multiple sclerosis.

The differential diagnosis between brain abscess and neoplasms (primary and secondary) is another challenge. These may appear as cystic lesions with rim enhancement on conventional MRI. Pyogenic abscess have high signal intensity in

diffusion weighted imaging, which is usually not seen in tumors. Nevertheless, some neoplasms may occasionally have restricted diffusion and biopsy is inevitable. In these cases, H-MRS may help to establish a diagnosis. If the VOI is positioned in the enhancing area, presence of Cho favors a neoplasm (Lai, 2008). If the VOI is positioned in the cystic area of a lesion, abscess and tumor both demonstrate high peak of lactate. Nonetheless, presence of acetate, succinate, and amino acids (AAs) such as valine, alanine, and leucine in the core of the lesion have high sensitivity for pyogenic abscess (Grand et al., 1999; Lai et al., 2002). These peaks are not seen in tumors. It is important to be aware that in patients with pyogenic brain abscess that are under antibiotic therapy these peaks may be absent.

H-MRS can also help in the differentiation of high grade gliomas from solitary metastasis. Both lesions show the same H-MRS pattern, with high Cho and low NAA. However, the high signal intensity on T2 weighted imaging seen in the perilesional area demonstrates elevated Cho/Cr ratio only in high grade gliomas (Fig. 30). This feature is consistent with the pathological findings of infiltrating tumor cells in areas of edema not seen in metastases(Law et al., 2002).

Gliomas are the most common and the most studied lesions among neuroepithelial tumors. They originate from glial cells (e.g. astrocytes or oligodentrocytes). Gliomas have an infiltrative nature resulting in neuronal cell damage and decreased NAA. Cohen et al. found decreased whole brain NAA in patients with glial tumors beyond the main tumor. This significant whole brain NAA depletion may reflect extensive tumor infiltration in the normal-appearing brain on MRI (Cohen et al., 2005). One quantitative MRS study (Stadlbauer et al., 2006) found a correlation between the percentage of tumor infiltration from the MRS-guided biopsy samples and changes in NAA, Cho, and Cho/NAA ratio in corresponding voxels. Absolute

concentration of NAA decrease, whereas absolute concentration of Cho, and Cho/NAA ratio increase with degree of tumor infiltration.

Astrocytomas can be classified into low grade (grade I and II, benign) and high grade (grade III and IV, malignant). High grade gliomas (anaplastic gliomas or grade III, and glioblastoma multiforme or grade IV) have higher Cho and lower NAA than low grade ones. Elevated Cho correlates with cellular proliferation and density. Although a number of studies in one systematic review (Hollingworth et al., 2006) have reported that MRS can accurately differentiate between low and high grade gliomas, the results of glioma grading by using MRS vary widely. These wide variations may be attributed to different methods and metabolites overlapping between different tumor grades. Statistically significant higher Cho/Cr, Cho/NAA, and relative cerebral blood volume (rCBV) in high grade than in low grade gliomas have been reported (Law et al., 2003), though, threshold values of metabolite ratios for grading of gliomas are not well established. Cho/Cr is the most frequently used ratio. Some institutions use a threshold value of 2.0 for Cho/Cr to differentiate low grade from high grade gliomas while some use a cutoff value of 2.5(Law et al., 2003).

As stated before, Lip and Lac peaks are absent under normal conditions. Lipid peak indicates necrosis in malignant tumors. Lac, a product of anaerobic glucolysis and accumulates in necrotic portions of tumors. Presence of Lip and Lac correlate with necrosis in high grade gliomas. Low grade gliomas show higher Myo levels compared with high grade gliomas (Castillo et al., 2000; Howe et al., 2003). This may be due to low mitotic index in low grade gliomas and, thus, lower mitogens (substances that trigger cell mitosis). Some mitogens can influence the metabolism of phosphatidylinositol, and Myo is also involved in formation of phosphatidylinositol. Thus, lack of phosphatidylinositol metabolism activation

results in Myo accumulation. Howe et al. concluded that high Myo was characteristic of grade II astrocytomas.

On serial MRS, malignant degeneration of gliomas can be detected by using percentage changes in Cho signal (Tedeschi et al., 1997). have demonstrated that interval percentage changes of Cho intensity in stable gliomas and progressive gliomas (malignant degeneration or recurrent disease) is less than 35 and more than 45, respectively. Interval increased Cho/Cr or Cho/NAA is suggestive of malignant progression.

Gliomatosis cerebri is a distinct entity of glial tumors. This rare disease is characterized by diffuse infiltration of glial cell neoplasm throughout the brain. Gliomatosis cerebri has various histological subtypes (astrocytoma, oligodendroglioma, or mixed glioma). The WHO classification denotes grades II, III and IV gliomatosis cerebri (Taillibert et al., 2006). Therefore patients with this tumor have a widely variable prognosis. Marked elevation of Myo and Cr has been found in gliomatosis cerebri and this may be attributed to glial activation rather than glial proliferation (Galanaud et al., 2003) because Cho level is moderately elevated, suggesting low glial cell density.

Oligodendroglioma is a subgroup of gliomas which has a better response to treatment (chemosensitive) and better prognosis than glioblastoma. This distinct tumor is devided into 2 groups according to the WHO classification: grades II and III. It originates from oligodendrocytes but often contains a mixed population of cells, particularly astrocytes. Loss of genes in chromosomes 1p and 19q is a characteristic genetic alteration of most oligodendrogliomas. On dynamic contrast-enhanced MR perfusion, low grade oligodendrogliomas may demonstrate high rCBV because they contain a dense network of branching capillaries (Lev et al.,2004). Thus a number of oligodendrogliomas can be misinterpreted as high

grade tumors because of their high rCBV which contributes to decrease reliability of rCBV in diffentiating the high vs. from low grade gliomas. Among the low grade gliomas, low grade oligodendrogliomas also exhibit significantly higher rCBV on dymamic-contrast MR perfusion (Cha et al., 2005). In groups of the oligodendroglial tumors, MRI studies have found that contrast enhancement is not suggestive of anaplasia as it is in astrocytomas. One study showed that rCBV was not significantly different between low and high grade oligodendroglimas (Xu et al., 2005). In contrast, another study (Spampinato et al., 2007), showed that rCBV was significantly different between low and high grade oligodendrogliomas.

The results of MRS studies in oligodendrogliomas are more consistent than those of MR perfusion studies. Similarly to astrocytomas, MRS of oligodendrogliomas demonstrates significantly higher Cho, Cho/Cr ratio, and a higher incidence of Lac and Lip in high grade than in low grade tumors (Rijpkema et al., 2003; Spampinato et al., 2007; Xu et al., 2005).

Nevertheless, low grade oligodendrogliomas may show highly elevated Cho, mimicking high grade tumors, because, these low grade tumors can have high cellular density but absent endothelial proliferation and necrosis (Spampinato et al., 2007). Apart from higher rCBV, the level of glutamine plus glutamate is significantly higher in low grade than in low grade astrocytomas and may help to distinguish these tumors from each other (Rijpkema et al., 2003).

Accurate grading of gliomas on the basis of MRS alone may be difficult. Combining MRS with conventional and other advanced MR imaging techniques such as perfusion MRI, grading becomes more precise. Some features of tumors on conventional MRI (e.g. contrast enhancement, surrounding edema, signal heterogeneity, necrosis, hemorrhage and midline crossing) and perfusion MRI (high rCBV) suggest a high grade. MRS is complementary and helpful for glioma

grading. High grade gliomas demonstrate marked elevation of Cho, decreased NAA and presence of Lac and Lip. Myo is high in low grade gliomas and decreases with increasing grades of tumors.

There is an important issue about post-radiation therapy in patients with brain tumors: differentiation between recurrent brain tumor and radiation injury/change, particularly when new contrast-enhancing lesions are seen in previously operated and/or irradiated regions. Many studies have found that Cho/Cr and/or Cho/NAA ratios are significantly higher in recurrent tumor (or predominantly tumor) than in radiation injury) (Rabinov et al., 2002; Smith et al., 2009; Weybright et al., 2005; Zeng et al., 2007).

One study (Zeng et al., 2007) reported that Lac/Cr ratio was significantly higher in recurrent tumor than in radiation injury whereas Lip/Cr ratio was significantly lower in recurrent tumor than in radiation injury. Another study showed that Lac or Lip signal alone was not helpful in differentiating these two conditions (Weybright et al., 2005). Rabinov et al. have also demonstrated no correlation between the signal intensity of Lip and the histopathology but they observed that Lac signal intensity in two patients with enhancing areas corresponding to recurrent tumor. It is probable that amount of Lip may be higher in an area of radiation changes than in tumor recurrence while Lac may be found in recurrent tumor but both Lip and Lac cannot differentiate these conditions.

2.3.12.2 Inborn Error of Metabolism

The diagnosis of an inborn error of metabolism is always challenging and mainly based on clinical and laboratorial findings, evolution, and genetic tests. Brain MRI may help narrowing the differential diagnosis, avoiding expensive genetic tests, or even establishing a final diagnosis. Since these disorders are caused by inherited enzymatic defects, concentrations of some metabolites may be abnormally low or

high. Metabolites with a very small concentration in brain tissue are not depicted on H-MRS. In these cases, the spectrum changes usually correspond to a general pathology, such as demyelination or ischemia. On some diseases, however, H-MRS may identify a specific biomarker that helps in the diagnosis (Barker et al, 2010).

Disorders that have specific H-MRS patterns may manifest as increase or absence of particular metabolites. Specific biomarkers can be seen in phenylketonuria (phenylalanine), Canavan disease (NAA), nonketotic hyperglycinemia (glycine), creatine deficiency (Cr), and maple syrup urine disease (branched-chain amino acids and keto acids) (van der Knapp and Valk, 2005).

Phenylalanine is an α-amino acid that is assigned at 7.36 ppm and can be used for diagnosis of phenylketonuria, follow up of treatment, and evolution of the disease. MRS is usually not needed because early diagnosis is made by neonatal screening tests and response to treatment can be monitored by phenylalanine blood levels and neuropsychological tests.

An increase of NAA signal is characteristic of Canavan disease (a disorder caused by a defect of the enzyme aspartoacylase that results in NAA accumulation in the brain) in a child with diffusely abnormal white matter and macrocephaly. However a high peak at 2.03 ppm is also noted in Salla disease, a rare autosomal recessive free sialic acid storage disorder (Varho et al., 1999). This latter disease accumulates acetylneuraminic acid (NANA), that resonances at the same frequency of NAA.

Nonketotic hyperglycinemia is an autosomal recessive disease that manifests mainly on neonatal period. There is accumulation of glycine in the brain and this metabolite shows up in H-MRS as a peak at 3.55 ppm. It is important to note that Myo resonates at 3.56ppm, therefore these peaks overlap. However, glycine has a

higher T2 value, and can be seen not only with short TE sequences but also with long TE (Barker et al, 2010). H-MRS is thus an important tool for diagnosing nonketotic hyperglycinemia and long TE studies must be acquired. H-MRS can also be used for monitoring the disease, correlating more with the clinical findings than blood and CSF glycine levels.

Maple syrup urine disease is an aminoacidopathy with accumulation of branched-chain α-keto and aminoacids. These metabolites resonate at 0.9 ppm, a region that is usually attributed to lipids. Lactate may also be present. In creatine deficiency there is a severe reduction of Cr peak. In both diseases, H-MRS may help with diagnosis and treatment.

All mitochondrial diseases caused by disorders of pyruvate metabolism, disorders of fatty acid oxidation, or defects of the respiratory chain and may have elevation of lactate on H-MRS. However, this finding is non-specific and lactate is not always present. Nonetheless, on mitochondrial disorders, abnormal lactate peak may be present when the VOI is positioned in normal brain parenchyma on MRI and in the ventricles (Bianchi et al., 2003; Cross et al., 1993). Therefore, even if the findings of H-MRS are non-specific they may be useful in the evaluation of mitochondrial disorders(Bianchi et al 2003).

2.4 Previous Studies:

comparing the diagnostic performance of MRS and stereotactic biopsy in the characterization of brain lesions, (Abdelaziz et al. 2016) testify that, MRS is a useful addition as it provides molecular information that assists in the characterization of various brain lesions; thus, MRS diagnosed neoplastic brain lesions in 15 cases (56%) and non-neoplastic brain lesions in 12 (44%).

In the assessment of progression and regression of brain tumors as well as monitoring of patient with primary tumors after therapy, (Lotumolo et al. 2016) testify that (MRS) showed better sensitivity, specificity, positive predictive value, negative predictive value and accuracy compared to diffusion weighted imaging (DWI).

(Anbarloui et al. 2015) state that MRS is a safe and informative tool in differentiating between tumor recurrence and radiation necrosis; moreover, sensitivity, specificity, and diagnostic accuracy of the algorithm for detecting tumor recurrence were 84%, 75% and 81%, respectively.

Significant differences were obtained in high-grade tumors for conventional MRS; in the same line, the presence of enhancement and necrosis were demonstrated to be the best predictors of high grade in primary brain tumors (sensitivity 95.9%; specificity 70%); and then, MRS is highly accurate in the assessment of tumor grade (Guzmán-De-Villoria 2014).

Proton MRS accurately predicted the pathological nature and clinical outcome of lesions in 15 out of 16 regions of interest (ROIs); in addition, it could assist in clinical decision making concerning patients potential for conducting stereotactic biopsy (Lin et al. 1999).

Considering the discriminatory power of MRS between a single tumor type and All Other tumors and between pairs of tumor types, MRS techniques further improve more features of MR spectra; definitely, this could be quantified reliably and MRS will be a powerful tool for preoperative diagnoses and for characterization of tumor metabolism in individual patients (Panigrahy et al.2006).

The presence of elevated choline and decreased NAA when using MRS is correlated with tumor histologic findings and may be used in distinguishing regions of viable cancer from normal and other noncancerous tissue, such as necrosis and astrogliosis; therefore, this suggests that MRS imaging may be valuable for guiding surgical biopsies and planning focal therapies (Dowling et al.2001)

(Sibtain A.et.al 2007) justify that, sometimes, MRS can increase the level of diagnostic confidence in which conventional MRI may be unhelpful and this could be noticed in three situations: (1) the distinction of high-grade gliomas and metastases from abscesses, (2) the assessment of tumour recurrence versus radiation necrosis, and (3) the identification of atypical meningiomas from typical meningiomas. In addition, MRS may add to the diagnostic certainty of histological diagnosis in some cases of meningioma, grade II astrocytoma and malignant aggressive lesions (gliomas and metastases) when conventional imaging is not characteristic. Thus, MRS may have a useful role in biopsy guidance, radiotherapy and surgical planning.

MRS is proposed in adjunction to MRI to help in the characterization of brain tumors by detecting metabolic alterations that may be indicative of the tumor class; based on that, MRS could be performed in clinical practice to guide the neurosurgeon into the most aggressive part of the lesions or to avoid unnecessary

surgery, which may furthermore decrease the risk of surgical morbidity(Callot et al.2008).

(Lee Sun Jin 2010) explain that, MRS ratios can be used to differentiate malignant and nonmalignant lesions from normal brain tissue. In general, high-grade astrocytoma have higher Cho/NAA and Cho/Cr ratios compared with low-grade astrocytoma. As a result, NAA is found in normal neurons and when altered, reductions occur both in tumors and in inflammatory lesions thereby indicating neuronal loss(Lee Sun Jin 2010).

MRS is now a- days considered as a main MRI investigation modality in the clinical routine jointly with conventional anatomical and functional magnetic resonance imaging for studying brain tumors. In fact, MRS provides complementary information about cellular metabolism. Actually, this allows differentiating the brain tumors from abscess.

Further, the MRS could be used in the therapeutic follow-up for evaluating the pathological active area of brain, and allows optimizing the guided biopsy as well as to differentiating recurrent tumor from a necrosis. The MR spectroscopy has a great interest in the exploration and therapeutic strategies of brain tumors. It allows a better general combination and confrontation of functional metabolism and morphological studies (Housni, Abdelkhalek et 2012).

MRS is a challenging technique and should only be used when pectral data will provide clinical information that is not obtained by other imaging techniques. The technique is very sensitive to inhomogeneities in the magnetic field and requires careful manual adjustment to ensure field uniformity. Recently, researchers and clinicians have considered the following: first, moved studies to higher field strengths to gain signal-to-noise ratio and to detect additional metabolites more reliably; second, implemented faster MRSI sequences to overcome low spatial

resolution and lengthy data acquisitions, and thirdly, they applied motion corrected MRS acquisitions (Currie, Stuart, et al.2011).

Gluch (2005) stated that *in vivo* applications of MRS have been developed, which aid in distinguishing malignant from normal tissues in brain tumors, breast, colon, cervix, esophageal, and prostate cancer reveal both the successes and failings of present technology. The author noted that verification that these non-invasive tests might supplant conventional histology in obtaining spatial diagnostic and chemical prognostic information remains for the time being illusive.

According to Jung and Westphalen (2012) studies have demonstrated that the addition of proton magnetic resonance spectroscopic imaging (1H-MRSI) to MR imaging improves tumor localization, volume estimation, staging, tissue characterization, and identification of recurrent disease after therapy. A recent multicenter study supported by the American College of Radiology Imaging Network, however, showed that the combination of 1H-MRSI and MR images does not improve tumor detection in patients with low-grade, low-volume disease selected to undergo radical prostatectomy. These results suggest that positive 1H-MRSI findings are more likely to reflect higher tumor grade and/or volume.

According to Shah et al (2006), "although MRS has mainly been used in diagnostics and tumor evaluation for brain tumors, it is becoming an increasingly important adjunct to conventional diagnostic and monitoring procedures for cancer of the prostate, colon, breast, cervix, pancreas, and esophagus. The clinical usefulness of MRS has yet to be fully substantiated".

Horska and Barker (2010) noted that the utility of MRS in diagnosis and evaluation of treatment response to human brain tumors has been widely documented. These researchers discussed the role of MRS in tumor classification, tumors versus non-neoplastic lesions, prediction of survival, treatment planning,

monitoring of therapy, and post-therapy evaluation. They concluded that there is a need for standardization and further study in order for MRS to become widely used as a routine clinical tool.

Guidelines on central nervous system cancers from the National Comprehensive Cancer Network (NCCN, 2016) state that magnetic resonance spectroscopy may be useful in anaplastic gliomas and glioblastoma

Chapter 3

Method & Material

3.1 Material

3.1.1 Patient

This study include (200) male and female with brain tumors their age ranged between 1-80 years refer to the department of radiology in royal care international hospital, for MR Spectroscopy examination , 190 pts comprises 95% are successfully diagnosed and included in the study. In 10 pts (5%) the diagnosis is equivocal and excluded from the sample.

3.1. 2 Machine

The study is carried out in Royal Care hospital in Khartoum State using MRI scanner of 1.5 Tesla- Toshiba advantage - made in Japan 2009 in the period from July 2014 – July 2017.

3.2 Method

3.2.1 Technique

(The following as Experimental and retrospective study for 200 BT patients (120 males, 80 females; age range, 1–80 years) who referred for MRI at Radiology Department at Royal Care Hospital in Sudan during 2014-2017, have been examined using MRI scanner of 1.5 tesla- Toshiba advantage- made in japan 2009. MRI protocol: All the cases were examined in supine position with standard circularly polarized head coil using the following sequences. Axial and Sagittal T1WI (550/8.7 ms) TR/TE spin echo. Coronal T2WI (5000/96 ms) TR/TE spin echo. l FALIR(Fluid Attenuation Inversion Recovery) (9000/92/ms) TR/TE spin echo. 5 mm section thickness,230 _ 230 Field of view (FOV) and 256 _ 256 matrix

size. There are(30 cases) cases which require contrast administration to confirm tumor diagnosis, intravenous administration of Gadolinium- DTPA, contrast enhanced T1WI in axial, sagittal and coronal planes was performed . About 70 cases with confirmed diagnosis MRS is done without contrast media.

After the identification of tumors by MRI technique we do the MRS image to know the type and nature of the tumor by using software program. This program is not found in all the MRI Department in Sudan and there is only at the Royal Care Hospital in Khartoum. The collected data is analyzed by using a point-resolved spectroscopic sequence (PRESS) with a volume of interest (VOI) between 1.5×1.5×1.5 cm3 (3.4 ml) and 2×2×2 cm3 (8 ml), depending on tumour size. The standard receiver head coil was used in all cases, and the spectroscopic exam was incorporated into a routine MR imaging study. The aim was to position the largest possible voxel within the solid tumoral area, avoiding areas of cysts, and with minimum contamination from the surrounding non-tumoral tissue. Automatic shimming of the linear X, Y and Z channels was used to optimize the field homogeneity.The water resonance was set on resonance and the water suppression pulse was optimized. Proton spectra were recorded with a repetition time of 2000 ms and an echo time of 136 ms .Assignment of the resonances of interest, including N-cetylaspartate At 2.02 ppm, creatine (Cr) at 3.03 ppm, choline (Cho) at 3.20 ppm, lipids (Lip 0.9) at 0.90 ppm and (Lip 1.3) at 1.30 ppm, glutamate and glutamine (Glx) at 2.35 ppm , lactate (Lact) at 1.35 ppm and to alanine(Ala) at 1.47 ppm. Data obtained were compared between tumour types in order to assess which findings were characteristic of each type and the utility of each metabolite resonance signal in classifying the different tumours. After the bring the biopsy to the laboratory this biopsy must be prepared for examination, it undergo treatment with different solution in steps cold processing.

Steps of tissue processing:

- Fixation: to preserve tissue structure from autolysis, done by 10% formal saline.
- Dehydration: removal of tissue water by ascending grades of ethanol(50%-70%-90%-absolute)
- Clearing: using xylene to remove alcohol.
- Impregnation &embedding using melted paraffin wax (65C) to solidify the tissue.
- Sectioning: cutting in thin sections(4microns) by microtome, then picked in slides.
- Staining of sections: routine stain is haemtoxylen and eosin (H&E stain) to stain nuclei blue and cytoplasm pink and other tissues a shade of red.
- The stained section covered and mounted with DPX for good contrast, then examined under the microscope for diagnosis.
- For harder tissues as bones, calcium must be remove first using EDTA or Nitric acid

3.2.2 Method of data analysis

The data will be analyzed using Excel (scatter plots depict the result of MRS and histopathology) and SPSS under windows

3.2.3 Significance of the study

This study will provide a Sudanese index (dimension) for brain tumors.

3.2.4 Ethical Consideration

There is no patient identification or individual patient details will be published. Also confidentiality will be ensured by making the collected data accessible only to the researcher and consultant radiologist and the head of radiology department. And also keep all data collected during the study will be stored on computer protected by password. All paper format data will be stored in locked cabinet.

Chapter 4

Result

4-1 Result

The following results highlighting the BTs in Sudan during the period of 2014-2017, incidence% based on gender, anatomical location, and variation incidence with aging, types of brain histopathology , the involved regions and the role of magnetic resonance spectroscopy .

Pt No	MRS Result	Histopathology Result		Pt No	MRS Result	Histopathology Result	
1	Malignant	Malignant		20	Malignant	Benign	*
2	Malignant	Malignant		21	Malignant	Malignant	
3	Malignant	Malignant		22	Benign	Benign	
4	Malignant	Malignant		23	Malignant	Malignant	
5	Benign	Benign		24	Malignant	Malignant	
6	Malignant	Malignant		25	Benign	Benign	
7	Malignant	Malignant		26	Benign	Benign	
8	Cystic	Benign	*	27	Benign	Benign	
9	Malignant	Malignant		28	Benign	Benign	
10	Malignant	Malignant		29	Malignant	Malignant	
11	Malignant	Malignant		30	Malignant	Malignant	
12	Benign	Benign		31	Malignant	Malignant	
13	Neoplastic tumor	Necrotic tumor	*	32	Malignant	Malignant	
14	Malignant	Malignant		33	Inflammation	Inflammatory	
15	Abscess	Abscess		34	Malignant	Malignant	
16	Benign	Malignant	*	35	Malignant	Malignant	
17	Malignant	Malignant		36	Malignant	Benign	*
18	Malignant	Malignant		37	Malignant	Malignant	
19	Malignant	Malignant		38	Benign	Benign	

Table 4: Demonstrate the correlation of histopathology with Magnetic Resonance Spectroscopy of human biopsies

Note (*) in table referred to deference between the MRS Results and Histopathology Results.

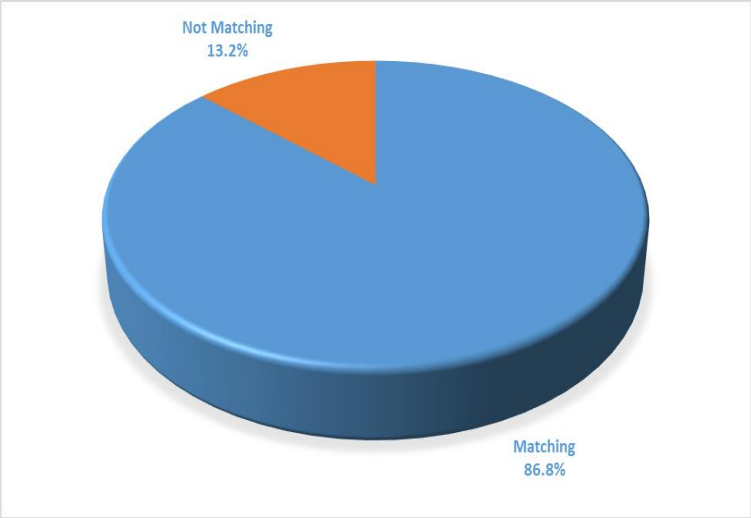

Figure 31. shows the percentage of results matching between the MRS and Histopathology results.

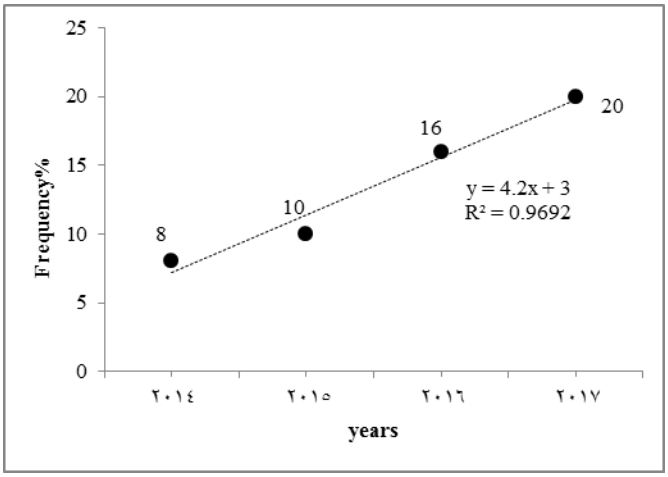

Figure 32. *Shows the incidence% of Brain tumors during the period 2014 - 2017*

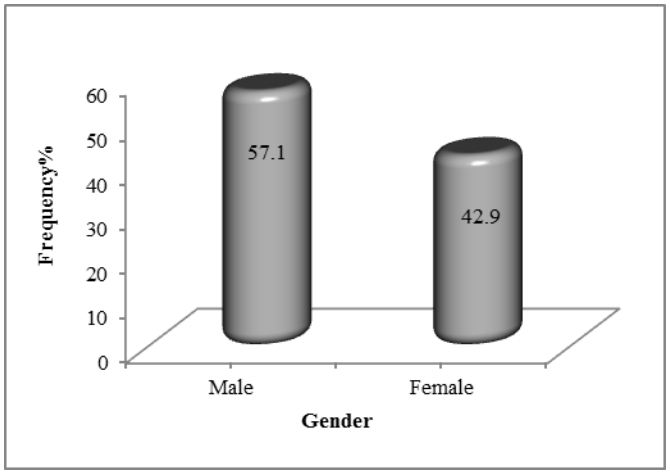

Figure 33. *Shows the brain tumors incidence % in Sudanese population during 2014-2017*

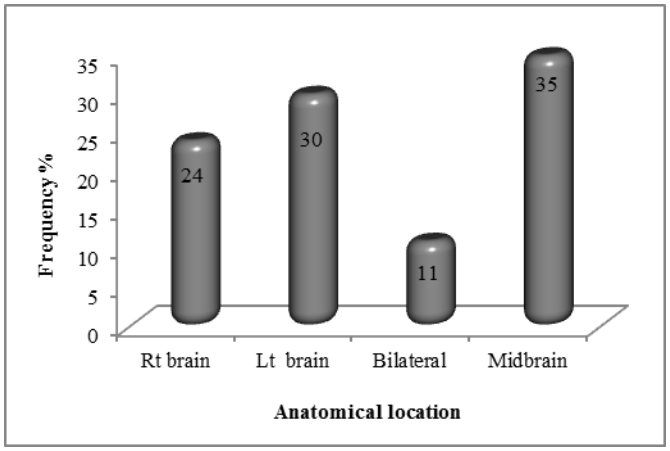

Figure 34. *Shows the anatomical sites involved by brain tumors during 2014-2017 in Sudan*

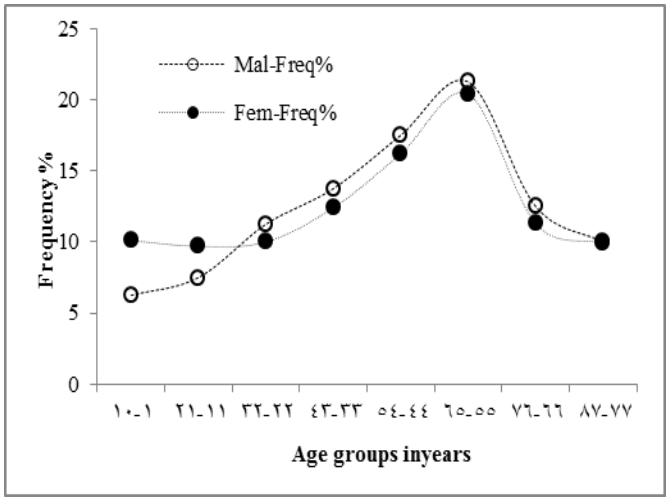

Figure 35. *Shows the brain tumors distribution in Sudanese population based on age group during 2014-2017.*

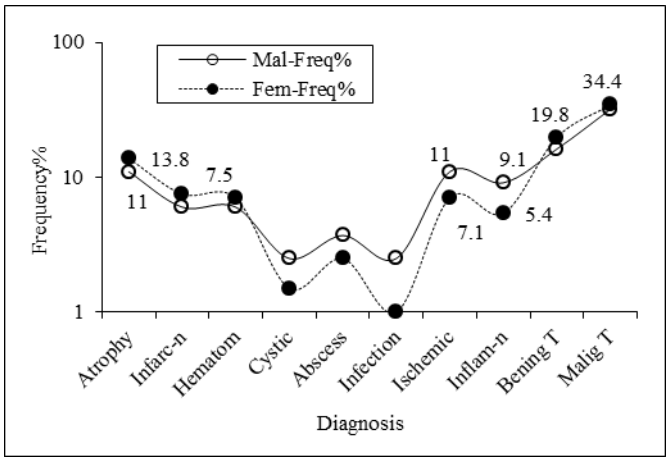

Figure 36. *Shows the types of brain pathologies in Sudanese population during 2014-2017.*

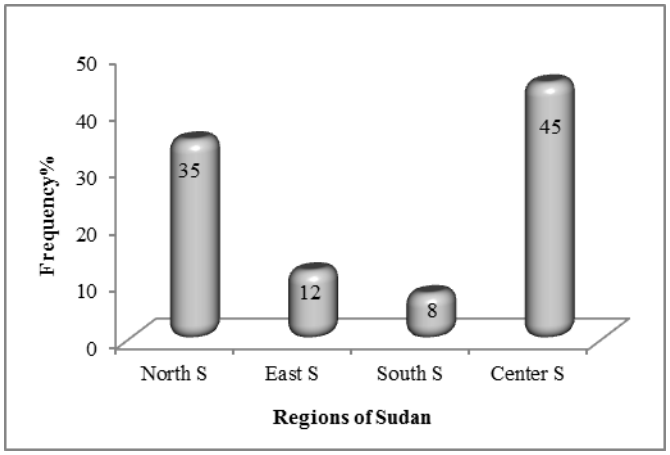

Figure 37. *Shows the distribution of brain tumors in different geographical sectors of Sudan (S)*

Chapter Five

Discussion, Conclusion & Recommendation

5-1 Discussion

The diagnostic study of BTs in Royal Care Hospital in Khartoum state using MRS showed little variation in view of accuracy relative to histological findings and our results similar to the Gold standard result in which MRS showed excellent diagnostic achievement relative to standard (histology) with accuracy 86.8% (Figure1).In all cases we find the elevation of Cho is seen in all neoplastic lesions. Cho peak may help with treatment response, diagnosis and progression of tumor. Its increase has been attributed to cellular membrane turnover which reflects cellular proliferation . Another H-MRS feature seen in brain tumors is decrease NAA. This metabolite is a neuronal marker and its reduction denotes destruction and displacement of normal tissue. Absence of NAA in an intra-axial tumor generally implies an origin outside of the central nervous system (metastasis) or a highly malignant tumor that has destroyed all neurons in that location. Cr signal, on the other hand, is slightly variable in brain tumors. It changes according to tumor type and grade. The typical H-MRS spectrum for a brain tumor is one of high level of Cho, low NAA and minor changes in Cr.As stated before, Lip and Lac peaks are absent under normal conditions. Lipid peak indicates necrosis in malignant tumors. Lac, a product of anaerobic glucolysis and accumulates in necrotic portions of tumors. Presence of Lip and Lac correlate with necrosis in high grade gliomas.. Lac/Cr ratio was significantly higher in recurrent tumor than in radiation injury whereas Lip/Cr ratio was significantly lower in recurrent tumor than in radiation injury(Zeng et al., 2007). Another study showed that Lac or Lip signal alone was not helpful in differentiating these two conditions (Weybright et al., 2005)..

The incidence% of Brain tumors during the period 2014 – 2017, presented the total tumors (*benign & malignant*) incidence (54%) from the total sample pathologies among 200 patients (Figure 2). It reveals clearly there was an increasing incidence annually by a factor of 7.2. Such results is quiet agreed with Greig et al, (Greig NH et al 1990) who reported that: the annual percentage increment of primary brain tumors among age groups (75-79, 80-84, and 85) were +7.0%, +20.4%, and +23.4% respectively. And it has been as a matter of debate whether such high incidence of diagnosed BTs ascribed to actual increased BTs incidence among the universe population or due to rapid diagnostic technologies development, but in Sudan the risk and etiological factors are present and the populations have been involving deeply in such factors.

The survey of brain tumors incidence% in Sudanese population during 2014-2017, revealed that: the male were the most gender involved by brain tumors as 57.1% relative to female (Figure 3). The high incidence of brain tumors among male ascribed to retinoblastoma protein (RB), which reducing cancer risk among male due to it is less activity and on the other hand the female are fewer incidences of brain tumors due to increase in active or less of retinoblastoma protein (Sun T et al 2014, Michael C. Purdy. 2014). As general BTs incidence increment has been ascribed to genetic factors accumulation (*inclusive family marriage*) and inherited altered genes (*EGFR amplification and mutation, amplification of CDK4 or MDM2, and deletion or mutation of TP53, RB, or PTEN*) which controlling cell cycle (*James, C.D et al 2002, Margaret Wrensch et al 2004*). In comparison with previous study; CBTRUS, (CBTRUS. 2005) also highlighted that: the brain tumors are so predominant among male with high incident in developed countries (*males, 5.8 and females, 4.1 per 100,000*) than in less developed countries (*males 3.0 and females 2.1 per 100,000*). As well as stated by Mackinny (McKinney P. A. (2004); where the male to female ratio was 1.5:1.0.

The incidence of BTs among both gender have specific anatomical location during 2014-2017 (Figure 4). In which the mid of the brain was the common involved anatomical segment by tumors which represents 35% followed by left brain (30%) and the right brain as (24%) and the least involved segment was bilateral i.e. both hemispheres of the brain. Such results are agreed with study done by Fatima,(Fatima Salih, S. 2011) in Sudan during the period 2009-2010, in which she found that: the anatomical brain tumor location in Sudanese patient were more in mid of the brain (46.7%), left brain (33.3%) and right (20%). The susceptibility of mid brain to tumorigenic could be ascribed or related to physiological hormonal changes by aging, gender, occupation and habits.

While the distribution of BTs based on age groups among Sudanese population during 2014-2017, showed that: the brain tumors have been encountered even during the age groups of 1-10 years old as common brain tumors among both gender and the incidence increases following the aging which peaking at 55-65 years old then decreased rapidly after; with general similar trend among both gender and through the entire ages (Figure 5). Similar trend of BTs being distributed based on age has been highlighted by Mackinny (McKinney P. A. (2004). However for 1-10 age group the common types were pediatric tumors that originated infratentorial (*Medduloblastoma, astrocytoma, Glioma and Craniphyringoma*) as mentioned by Wilson and Mosely, (Wilson J.L, I.F. Mosely. 1978), while among adult; were commonly as metastasis from breast, cervix, prostate and nasopharyngeal cancers. The general picture of BTs showed that: benign tumors are more predominant among adult female; that could be ascribed to hormonal levels fluctuation and response to chemotherapy administration for several chronic inflammation, while malignant ones have been predominated among male adult.

The BTs have different types in view of histology; in Sudanese population during 2014-2017 the common pathologies of brain were atrophy and infarction that represents 13.8% and 7.2% respectively; however among these groups the impact of diabetes on brain and other vital anatomical structures as well as aging effect (Hughes, T.M et al 2013- Mohammed A. Ali Omer et al 2014) increases the incidence of atrophy among adult. Then the pathologies incidence decreased for hematoma, cystic, abscess and infection while the incidence increases obviously among male and female for ischemic (11%, 7.1%), inflammation (9.1%, 5.4%), benign tumors (19.8%) and malignant tumors (34.4%) as in Figure (6). The possible causes for such results could be ascribed to extensive usage of underground water which is contaminated with sewage and wastewater for drinking (self-survey results). Also could be due to contamination by nitrate and nitrite compounds that leeching into drinking water supplies (Mueller BA et al 2001, Steindorf K et al 1994) in addition to exposure to low-level radiofrequencies as accepted approved carcinogenesis (Moulder JE et al 2006).

The geographical distribution of BTs in different sectors of Sudan to some extend has a link with the risk factors and accordingly the the center of Sudan and North of Sudan were the most endemic sectors by BTs relative to other sectors; which represented 45% and 35% respectively, then east and south of Sudan represented 12% and 8% respectively (Figure 7). Indeed the distribution of BTs in Sudan seemed to be dependent on the population (5.2 million in 2014), aging factors: most are young adult and old ones, food and dietary factors: as has been approved that N-nitroso compounds could induce neurosarcomas and potent neurocarcionogenic (Dietrich, M., Block et al 2005, Yun Zhu et al 2014); in this realm Sudanese population have focused on processed meat and fast food intake abundantly, occupational and the living style: as exposed workers to electric and magnetic fields showed significant (10% to 20%) risk increment for brain tumors

(Zhuoyu Sun et al 2014, Kheifets L I et al1995); in addition to the technology of communication specially wireless exemplar in cellular phones and electromagnetic field utilized in medical field (*magnetic resonance imaging*) as have been approved to induce certain brain vacuolation, atrophied hepatocytes, spleen and kidney rupture (Hans-Olov et al 2008). Relative to this facts: Sudanese population randomly living near high tension transformer/towers of electricity, wireless station and uncontrolled usage of cell phone (*long duration chatting*) that may contribute in increasing the risk factors and incidence of BTs.

5-2 Conclusion

Magnetic Resonance Spectroscopy (MRS) is now a days considered as a main MRI investigation modality in the clinical routine jointly with conventional anatomical and functional magnetic resonance imaging for studying brain tumors. MRS provides complementary information about cellular metabolism. This allows differentiating the brain tumors from abscess, the diagnosis of the tumor type, characterization of brain tumors, as well as local study of the morphological abnormalities observed in conventional MRI. The MRS could be used in the therapeutic follow-up for evaluating the pathological active area of brain, and allows optimizing the guided biopsy as well as to differentiating recurrent tumor from a necrosis. The MR spectroscopy has a great interest in the exploration and therapeutic strategies of brain tumors. It allows a better general combination and confrontation of functional metabolism and morphological studies.

1H-MRS technique can aid in the management of cancer patients, serving as a noninvasive biomarker of metabolism in tumors. 1H-MRS has achieved great strides as a molecular imaging technique since its introduction, and its scope in many clinical scenarios and research settings is rising. MRS allowed the noninvasive differentiation between high-grade and low grade tumors. Cho/NAA, Cho/Cr as well as Cho+Cr/NAA ratios were the most reliable in determining the tumor grade. MR spectroscopy techniques further improve, more features of MR spectra can be quantified reliably and MR spectroscopy will be a powerful tool for preoperative diagnoses and for characterization of tumor metabolism in individual patients. MRS can also be performed in clinical practice to guide the neurosurgeon into the most aggressive part of the lesions or to avoid unnecessary surgery, which may furthermore decrease the risk of surgical morbidity.

MRS is a challenging technique and should only be used when spectral data will provide clinical information that is not obtained by other imaging techniques. The technique is very sensitive to inhomogeneities in the magnetic field and requires careful manual adjustment to ensure field uniformity. Artifacts can arise from braces on teeth or proximity to sinuses. If any bone is included in the voxel, it can cause artifacts due to the lipid signal arising from bone marrow. Because of the smaller voxel size and limitations in the length of time of image acquisition, MRSI data is noisier than single voxel MRS. MRS is also very sensitive to motion. To overcome these limitations of MRS, researchers and clinicians have moved studies to higher field strengths to gain signal-to-noise ratio and to detect additional metabolites more reliably.

5-3 Recommendations

- MRS should be done routinely in patients with brain lesions to improve the accuracy of neuro diagnosis
- Increase the number of diagnostic centers using magnetic resonance spectroscopy technique
- MRS as a noninvasive examination can be repeated with no risk to the patient.
- A local study to compare the diagnosis obtained from MRI+MRS against histopathological diagnosis to determine sensitivity and specificity of brain MRS in our local setup.
- Performing brain MRS as part of a complete MRI examination for any intracranial mass lesion where MRI alone is inconclusive, and the indication is appropriate as deemed by the radiologist; preferably at no additional cost to the patient; and at the same sitting as the initial MRI examination. Increasing the number of MRS examinations performed will greatly help bring down the cost to the patient
- Finally, we should encourage more studies to be done in MRS with a larger sample size and comparison with other imaging and histopathology findings to give us more information about the impact of the new technique MRS in our diagnosis and to help us to adhere to the discipline of evidence based medicine.

References :

-Abdelaziz, O., Eshra, M., Belal, A., & Elshafei, M. (2016). Diagnostic value of magnetic resonance spectroscopy compared with stereotactic biopsy of intra-axial brain lesions. *Journal of Neurological Surgery Part A: Central European Neurosurgery*, *77*(04), 283-290.

-Alireza Baratloo, Mostafa Hosseini, Ahmed Negida, Gehad El Ashal. (2015). Part 1: Simple Definition and Calculation of Accuracy, Sensitivity and Specificity. Emergency (2015); 3 (2): 48-49.

-Anbarloui, M. R., Ghodsi, S. M., Khoshnevisan, A., Khadivi, M., Abdollahzadeh, S., Aoude, A., ... & Faghih-Jouibari, M. (2015). Accuracy of magnetic resonance spectroscopy in distinction between radiation necrosis and recurrence of brain tumors. *Iranian journal of neurology*, *14*(1), 29.

-Arslanoglu A, Bonekamp D, Barker PB, Horská A. (2004). Quantitative proton MR spectroscopic imaging of the mesial temporal lobe. *J*

-Baker EH, Basso G, Barker PB, Smith MA, Bonekamp D, Horská A. (2008). Regional apparent metabolite concentrations in young adult brain measured by (1)H MR spectroscopy at 3 Tesla. *J Magn Reson Imaging* 27:489-499.

-Barker, PB; Bizzi, A; De Stefano, N; Gullapalli, R & Lin, DDM. (2010). *Clinical MR Spectroscopy* (1st edition), Cambridge University Press, ISBN 9780521868983, New York, United States of America.

-Benard F, Romsa J, Hustinx R. Imaging gliomas with positron emission tomography and single-photon emission computed tomography. Semin Nucl Med 2003; 33: 148-162.

-Bertholdo, Débora, Arvemas Watcharakorn, and Mauricio Castillo. (2013) "Brain proton magnetic resonance spectroscopy: introduction and overview." Neuroimaging Clinics of North America 23.3: 359-380.

-Bianchi MC, Tosetti M, Battini R, Manca ML, Mancuso M, Cioni G, Canapicchi R, Siciliano G. (2003) Proton MR spectroscopy of mitochondrial diseases: analysis of brain metabolic abnormalities and their possible diagnostic relevan *AJNR Am J Neuroradiol.* 24(10):1958- 66.

-Bitsch A, Bruhn H, Vougioukas V, Stringaris A, Lassmann H, Frahm J & Brück W. (1999). Inflammatory CNS demyelination: histopathologic correlation with in vivo quantitative proton MR spectroscopy. *AJNR Am J Neuroradiol.* 20(9):1619-27.

-Bosc, Romain, Rene Olivier Mirimanoff, and Mahmut Ozsahin, eds. (2011) *Management of rare adult tumours*. Springer Science & Business Media.

-Buckner, J. C., Brown, P. D., O'neill, B. P., Meyer, F. B., Wetmore, C. J., & Uhm, J. H. (2007, October). Central nervous system tumors. In *Mayo Clinic Proceedings* (Vol. 82, No. 10, pp. 1271-1286). Elsevier

-Cady, Ernest B. (2012) *Clinical magnetic resonance spectroscopy*. Springer Science & Business Media.

-Callot, V., Galanaud, D., Le Fur, Y., Confort-Gouny, S., Ranjeva, J. P., & Cozzone, P. J. (2008). 1 H MR spectroscopy of human brain tumours: a practical approach. *European journal of radiology*, *67*(2), 268-274.

-Castillo M, Smith JK, Kwock L. (2000). Correlation of myo-inositol levels and grading of cerebral astrocytomas. *AJNR Am J Neuroradiol*. Oct;21(9):1645-9. National Comprehensive Cancer Network (NCCN).(2016) Central nervous system

cancers. NCCN Clinical Practice Guidelines in Oncology, version 1.2016. Fort Washington, PA: NCCN.

-Central Brain Tumor Registry of the United States (CBTRUS). (2005). Statistical Report: Primary brain tumors in the United States, 1998–2002. Hinsdale, IL: Central Brain Tumor Registry of the United States.

-Cha S, Tihan T, Crawford F, Fischbein NJ, Chang S, Bollen A, Nelson SJ, Prados M, Berger MS, Dillon WP. (2005). Differentiation of low-grade oligodendrogliomas from low-grade astrocytomas by using quantitative blood-volume measurements derived from dynamic susceptibility contrast-enhanced MR imaging. *AJNR Am J Neuroradiol*. Feb;26(2):266-73.

-Chandana SR, Movva S, Arora M, Singh T. (2008). Primary brain tumors in adults." American family physician. 77(10): 1423-1430. PMID: 18533376.

-Chang L, Ernst T, Poland RE, Jenden DJ. (1996). In vivo proton magnetic resonance spectroscopy of the normal aging human brain. *Life Sci* 58:2049-2056.

-Charles HC, Lazeyras F, Krishnan KR, Boyko OB, Patterson LJ, Doraiswamy PM, McDonald WM. (1994). Proton spectroscopy of human brain: effects of age and sex. *Prog Neuropsychopharmacol Biol Psychiatry* 18:995-1004.

-Christiansen P, Toft P, Larsson HB, Stubgaard M, Henriksen O. (1993). The concentration of N-acetyl aspartate, creatine + phosphocreatine, and choline in different parts of the brain in adulthood and senium. *Magn Reson Imaging* 11:799-806.

-Cohen BA, Knopp EA, Rusinek H, Babb JS, Zagzag D, Gonen O. (2005). Assessing global invasion of newly diagnosed glial tumors with whole-brain proton MR spectroscopy. *AJNR Am J Neuroradiol*. Oct;26(9):2170-7.

-Cross JH, Gadian DG, Connelly A, Leonard JV. (1993). Proton magnetic resonance spectroscopy studies in lactic acidosis and mitochondrial disorders. *J Inherit Metab Dis.* 16(4):800-11.

-Currie, S., Hadjivassiliou, M., Craven, I. J., Wilkinson, I. D., Griffiths, P. D., & Hoggard, N. (2012). Magnetic resonance spectroscopy of the brain. *Postgraduate medical journal*, postgradmedj-2011.

-De Moor, J. S., Mariotto, A. B., Parry, C., Alfano, C. M., Padgett, L., Kent, E. E., ... & Rowland, J. H. (2013). Cancer survivors in the United States: prevalence across the survivorship trajectory and implications for care. Cancer Epidemiology and Prevention Biomarkers, 22(4), 561-570.

-De Stefano N, Filippi M, Miller D, Pouwels PJ, Rovira A, Gass A, Enzinger C, Matthews PM & Arnold DL. (2007). Guidelines for using proton MR spectroscopy in multicenter clinical MS studies. *Neurology.* 13;69(20):1942-52.

-Degaonkar MN, Pomper MG, Barker PB. (2005). Quantitative proton magnetic resonance spectroscopic imaging: regional variations in the corpus callosum and cortical gray matter. *J Magn Reson Imaging* 22:175-179.

-Dezortova M, Hajek M. (2008). (1)H MR spectroscopy in pediatrics. *Eur J Radiol* 67:240-249.

-Dietrich, M., Block, G., Pogoda, J. M., Buffler, P., Hecht, S., & Preston-Martin, S. (2005). A review: Dietary and endogenously formed N-nitroso compounds and risk of childhood brain tumors. *Cancer Causes and Control. 16*(6), 619-635. DOI: 10.1007/s10552-005-0168-y.

-Dowling, C., Bollen, A. W., Noworolski, S. M., McDermott, M. W., Barbaro, N. M., Day, M. R., ... & Vigneron, D. B. (2001). Preoperative proton MR spectroscopic imaging of brain tumors: correlation with histopathologic analysis of resection specimens. American Journal of Neuroradiology, 22(4), 604-612.

-Duyn JH, Moonen CT (1993). Fast proton spectroscopic imaging of human brain using multiple spin-echoes. *Magn Reson Med* 30:409–414

-Duyn JH, Gillen J, Sobering G, van Zijl PC, Moonen CT (1993) Multisection proton MR spectroscopic imaging of the brain. *Radiology* 188:277–282.

-El-Dahshan, E. S. A., Hosny, T., & Salem, A. B. M. (2010). Hybrid intelligent techniques for MRI brain images classification. Digital Signal Processing, 20(2), 433-441.

-Ethofer T, Mader I, Seeger U, Helms G,Erb M, Grodd W, Ludolph A, Klose U(2003) Comparison of longitudinal metabolite relaxation times in different regions of the human brain at 1.5 and 3 Tesla. *Magn Reson Med* 50:1296–1301.

-Fatima Salih, S. (2011). Brain Tumors among Sudanese Patients (A histopathological Study) (Doctoral dissertation, U of K), Sudan.

-Fayed N, Olmos S, Morales H, Modrego PJ. (2006). Physical basis of magnetic resonance spectroscopy and its application to central nervous system diseases. *Am J Applied Sci* 3:1836-1845.

-Fayed, Nicolás, and Pedro J. Modrego. (2005) "The contribution of magnetic resonance spectroscopy and echoplanar perfusion-weighted MRI in the initial assessment of brain tumours." Journal of neuro-oncology 72.3: 261-265.

-Fehrenbach, Margaret J., and Susan W. Herring.(2015) Illustrated Anatomy of the Head and Neck-E-Book. Elsevier Health Sciences.

-Fernando KT, McLean MA, Chard DT, MacManus DG, Dalton CM, Miszkiel KA, Gordon RM, Plant GT, Thompson AJ & Miller DH. (2004). Elevated white matter myo-inositol in clinically isolated syndromes suggestive of multiple sclerosis. *Brain* 127(Pt 6):1361-9.

-Galanaud D, Chinot O, Nicoli F, Confort-Gouny S, Le Fur Y, Barrie-Attarian M, Ranjeva JP, Fuentès S, Viout P, Figarella-Branger D, Cozzone PJ. (2003). Use of proton magnetic resonance spectroscopy of the brain to differentiate gliomatosis cerebri from low-grade glioma. *J Neurosurg*. Feb;98(2):269-76.

-Gao, H., Yang, Z., Cao, S., Xiong, Y., Zhang, S., Pang, Z., & Jiang, X. (2014). Tumor cells and neovasculature dual targeting delivery for glioblastoma treatment. Biomaterials, 35(7), 2374-2382.

-Gill, S. K., Panigrahy, A., Arvanitis, T. N., & Peet, A. C. (2013). Magnetic resonance spectroscopy of pediatric brain tumors. In MR Spectroscopy of Pediatric Brain Disorders (pp. 45-60). Springer New York.

-Gluch L. (2005)Magnetic resonance in surgical oncology: II - literature review. ANZ J Surg. 2005;75(6):464-470.

-Grand S, Passaro G, Ziegler A, Estève F, Boujet C, Hoffmann D, Rubin C, Segebarth C, Décorps M, Le Bas JF, Rémy C. (1999). Necrotic tumor versus brain abscess: importance of amino acids detected at 1H MR spectroscopy-initial results. *Radiology*. 213(3):785-93.

-Greig NH, Ries LG, Yancik R, Rapoport S. I. (1990). Increasing annual incidence of primary malignant brain tumors in the elderly. J. Natl. Cancer Inst. 82(20):1621-4. PMID: 2213902.

-Grover, V. P., Tognarelli, J. M., Crossey, M. M., Cox, I. J., Taylor-Robinson, S. D., & McPhail, M. J. (2015). Magnetic resonance imaging: principles and techniques: lessons for clinicians. Journal of clinical and experimental hepatology, 5(3), 246-255.

-Gupta, Rakesh K., and Robert B. Lufkin, eds. 2002. MR imaging and spectroscopy of central nervous system infection. Kluwer Academic Publishers.

-Guzmán-De-Villoria, J. A., Mateos-Pérez, J. M., Fernández-García, P., Castro, E., & Desco, M. (2014). Added value of advanced over conventional magnetic resonance imaging in grading gliomas and other primary brain tumors. *Cancer Imaging*, *14*(1), 35.

-Haga KK, Khor YP, Farrall A , Wardlaw JM. (2009). A systemic review of brain metabolite changes, measured with (1)H magnetic resonance spectroscopy, in healthy aging. *Neurobiol Aging* 30:353-363

-Hajek M, Dezortova M. (2008). Introduction to clinical in vivo MR spectroscopy. *Eur J Radiol* 67:185-193.

-Hans-Olov Adami, David Hunter, Dimitrios Trichopoulos. (2008). Textbook of Cancer Epidemiology, 2nd. edition, Oxford University Press, New York – USA.

-Heimer, Lennart.(2012) The human brain and spinal cord: functional neuroanatomy and dissection guide. Springer Science & Business Media.

-Henning, A. (2008). Magnetic resonance spectroscopy localization at high and ultra-high field strength (Doctoral dissertation).

-Hetherington HP, Mason GF, Pan JW, Ponder SL, Vaughan JT, Twieg DB, Pohost GM. (1994). Evaluation of cerebral gray and white matter metabolite differences by spectroscopic imaging at 4.1T. *Magn Reson Med* 32:565-571.

-Hollingworth W, Medina LS, Lenkinski RE, Shibata DK, Bernal B, Zurakowski D, Comstock B, Jarvik JG. (2006). A systematic literature review of magnetic resonance spectroscopy for the characterization of brain tumors. *AJNR Am J Neuroradiol.* Aug;27(7):1404-11.

-Horner, M. J., Ries, L. A. G., Krapcho, M., Neyman, N., Aminou, R., Howlader, N., ... & Miller, B. A. (2009). SEER Cancer Statistics Review, 1975-2006, National Cancer Institute. Bethesda, MD.

-Horská, Alena, and Peter B. Barker. (2010)"Imaging of brain tumors: MR spectroscopy and metabolic imaging." *Neuroimaging clinics of North America* 20.3: 293-310.

-Housni, Abdelkhalek, and Saïd Boujraf. (2012) "Magnetic resonance spectroscopy in the diagnosis and follow-up of brain tumors." *Journal of Biomedical Science and Engineering* 5.12: 853.

-Howe FA, Barton SJ, Cudlip SA, Stubbs M, Saunders DE, Murphy M, Wilkins P, Opstad KS, Doyle VL, McLean MA, Bell BA, Griffiths JR. (2003). Metabolic profiles of human brain tumors using quantitative in vivo 1H magnetic resonance spectroscopy. *Magn Reson Med.* Feb;49(2):223-32.

-Howe, Franklyn A., and Kirstie S. Opstad. (2003) "1H MR spectroscopy of brain tumours and masses." NMR in Biomedicine 16.3: 123-131.

-Hughes, T.M., C.M. Ryan, H.J. Aizenstein, et al. (2013). Frontal gray matter atrophy in middle aged adults with type 1 diabetes is independent of cardiovascular risk factors and diabetes complications. J. Diab. Compl. 27: 558–564.

-Huile Gao, Xinguo Jiang. (2013). Progress on the diagnosis and evaluation of brain tumors. Cancer Imaging (2013) 13(4), 466-481. DOI: 10.1102/1470-7330.2013.0039.

-Hussein S. Abu-Salih and Ali M. Abdul-Rahman. (1988). Tumors of the brain in the Sudan. Surgical Neurology. 3:194-196. DOI: 10.1016/0090-3019 (88) 90005-5.

-Hutter A, Schwetye KE, Bierhals AJ, McKinstry RC. 2003 Brain neoplasms: epidemiology, diagnosis, and prospects for cost-effective imaging. Neuroimaging Clin N Am.; 13: 237-250.

-Intisar E Saeed, Hsin-Yi Weng, Kamal H Mohamed, and Sulma I. Mohammed. (2014). Cancer incidence in Khartoum, Sudan: first results from the Cancer Registry, 2009–2010. Cancer Med. 3(4): 1075–1084. DOI: 10.1002/cam4.254.

-Jacobs MA, Horská A, van Zijl PC, Barker PB. (2001). Quantitative proton MR spectroscopic imaging of normal human cerebellum and brain stem. *Magn Reson Med* 46:699-705.

-James, C.D., Smith, J.S., and Jenkins, R.B. (2002). Genetic and molecular basis of primary central nervous system tumors. In: Levin, V. (Ed.), *Cancer in the Nervous System.* 2nd. Edition, New York: Oxford University Press. pp. 239-251.

-Joseph Timmons. (2012). Primary Brain Tumors – Everything a Medical Student Needs to Know. Scottish Universities Medical Journal, Dundee; 1(1): 31-37.

Jung AJ, Westphalen AC(2012). Imaging prostate cancer. Radiol Clin North Am.; 50(6).

-Karak, A.K., Singh, R., Tandon, P.N., and Sarkar, C. (2000). A comparative survival evaluation and assessment of interclassi.cation concordance in adult supratentorial astrocytic tumors. Pathol. Oncol. Res. 6, 46-52.

-Kheifets L I, Afifi A A, Buffler P A, Zhang Z W, (1995). Occupational electric and magnetic field exposure and brain cancer: a meta-analysis. J. Occup. Environ Med. 35:1327-41.

-Kounelakis, M. G., Zervakis, M. E., Blazadonakis, M. E., Postma, G. J., Buydens, L. M. C., Heerschap, A., & Kotsiakis, X. (2008). Feature Selection for Brain Tumour Classification using Ratios of Metabolites' Peak Areas from MRSI Data. In 6th European Symposium on Biomedical Engineering ESBME, Chania, Greece (pp. 1-6).

-Kreis R, Ernst T, Ross BD. (1993a). Absolute quantitation of water and metabolites in the human brain. II. Metabolite concentrations. *J Magn Reson Ser B* 102:9-19.

-Kreis R, Ernst T, Ross BD. (1993b). Development of the human brain: In vivo quantification of metabolite and water content with proton magnetic resonance spectroscopy. *Magn Reson Med* 30:424-437.

-Kwabi-Addo, Bernard, and Tia Laura Lindstrom.(2011) Cancer Causes and Controversies: Understanding Risk Reduction and Prevention: Understanding Risk Reduction and Prevention. ABC-CLIO.

-Lai PH, Ho JT, Chen WL, Hsu SS, Wang JS, Pan HB, Yang CF. (2002). Brain abscess and necrotic brain tumor: discrimination with proton MR spectroscopy and diffusion-weighted imaging. *AJNR Am J Neuroradiol*. Sep;23(8):1369-77.

-Lai PH, Weng HH, Chen CY, Hsu SS, Ding S, Ko CW, Fu JH, Liang HL, Chen KH.(2008) In vivo differentiation of aerobic brain abscesses and necrotic glioblastomas multiforme using proton MR spectroscopic imaging. *AJNR Am J Neuroradiol*. 29(8):1511-8.

-Landis, S. H., Murray, T., Bolden, S., & Wingo, P. A. (1999). Cancer statistics, 1999. CA: A cancer Journal for Clinicians, 49(1), 8-31.

-Iannelli, G., Caivano, R., Rago, L., Simeon, V., Lotumolo, A., Rabasco, P., ... & Panebianco, V. (2016). Diffusion-weighted magnetic resonance imaging in patients with prostate cancer treated with radiotherapy. *Tumori*, *102*(1), 71-76.

-Law M, Cha S, Knopp EA, Johnson G, Arnett J, Litt AW. (2002). High-grade gliomas and solitary metastases: differentiation by using perfusion and proton spectroscopic MR imaging. *Radiology*. 222(3):715-21.

-Law M, Yang S, Wang H, Babb JS, Johnson G, Cha S, Knopp EA, Zagzag D. (2003). Glioma grading: sensitivity, specificity, and predictive values of perfusion MR imaging and proton MR spectroscopic imaging compared with conventional MR imaging. *AJNR Am J Neuroradiol.* Nov-Dec;24(10):1989-98.

-Lee, Sun Jin.(2010) "Proton MR spectroscopy of brain tumors: The cause of wrong diagnosis and grading." European Congress of Radiology 2010

-Lev MH, Ozsunar Y, Henson JW, Rasheed AA, Barest GD, Harsh GR 4th, Fitzek MM, Chiocca EA, Rabinov JD, Csavoy AN, Rosen BR, Hochberg FH, Schaefer PW, Gonzalez RG. (2004). Glial tumor grading and outcome prediction using

dynamic spin-echo MR susceptibility mapping compared with conventional contrast-enhanced MR: confounding effect of elevated rCBV of oligodendrogliomas [corrected]. *AJNR Am J Neuroradiol*. Feb;25(2):214-21.

-Lim KO, Spielman DM. (1997). Estimating NAA in cortical gray matter with applications for measuring changes due to aging. *Magn Reson Med* 37:372-377.

-Lin A, BlS, Mamelak AN(1999). Efficacy of proton magnetic resonance spectroscopy in clinical decision making for patients with suspected malignant brain tumors. J Neurooncol.;45(1):69-81.

-Louis, David N., et al. (2016) "The 2016 World Health Organization classification of tumors of the central nervous system: a summary." Acta neuropathologica 131.6: 803-820.

-Magalhaes A, Godfrey W, Shen Y, Hu J, Smith W.2005. Proton magnetic resonance spectroscopy of brain tumors correlated with pathology. Acad Radiol.; 12: 51-57.

-Margaret Wrensch, Yuriko Minn, Terri Chew, Melissa Bondy, and Mitchel S. Berger. (2002). Epidemiology of primary brain tumors: Current concepts and review of the literature. Neuro-Oncology. 4: 278–299.

-Majós C, Aguilera C, Alonso J, Julià-Sapé M, Castañer S, Sánchez JJ, Samitier A, León A, Rovira A & Arús C. (2009). Proton MR spectroscopy improves discrimination between tumor and pseudotumoral lesion in solid brain masses. *AJNR Am J Neuroradiol*. 30(3):544-51.

-Majós C, Julià-Sapé M, Alonso J, Serrallonga M, Aguilera C, Acebes JJ, Arús C & Gili J. (2004). Brain tumor classification by proton MR spectroscopy: comparison of diagnostic accuracy at short and long TE. *AJNR Am J Neuroradiol.* 10:1696-704.

-Mandal, Pravat K. (2012) "In vivo proton magnetic resonance spectroscopic signal processing for the absolute quantitation of brain metabolites." *European Journal of Radiology* 81.4: e653-e664.

-McKnight, T. R. (2004, October). Proton magnetic resonance spectroscopic evaluation of brain tumor metabolism. In Seminars in oncology (Vol. 31, No. 5, pp. 605-617). WB Saunders.

-McKinney, P A. (2004). Brain tumors: incidence, survival, and aetiology. Journal of neurology, neurosurgery and psychiatry; 75(2): 12-17. DOI: 10.1136/jnnp.2004.040741.

-Michael C. Purdy. (2014). Study reveals one reason brain tumors are more common in men. Washington University School of Medicin.

https://source.wustl.edu/2014/08/study-reveals-one-reason-brain-tumors-are-more-common-in-men/ (July 13, 2017).

-Mohammed A. Ali Omer, Emad M. Mukhtar Alasar, Mohamed E. M. Gar-elnabi, Ghada A. E. Sakin, Yahia M. Bushara. (2014). Measurement of Cranial and Brain Ventricle Volumes Relative to Pathologies. International Journal of Science and Research (IJSR) 3(5): 987-991.

-Mohammed A. Ali Omer, Ayman H. Eljack1, Mohamed E. M. Gar-alnabi, Mustafa Z. Mahmoud, Muatasim Elseid, Ghada A. Edam. (2014-b). Ultrasonographic Characteristics of Diabetes Impacts in Kidneys' Morphology,

Open Journal of Radiology. 4, 301-308. DOI:10.4236/ojrad.2014.44039.

-Mohamed E.M. Saeed, Jingming Cao, Babikir Fadul, Onat Kadioglu, Hassan E. Khalid, Zahir Yassin, Siddig M. Mustafa, Elfatih Saeed and Thomas Efferth. (2016). A Five-year Survey of Cancer Prevalence in Sudan. Anticancer Research 36: 279-286. PMID: 26722054.

-Moser HW, Barker PB.(2005) Magnetic resonance spectroscopy: A new guide for the therapy of adrenoleukodystrophy. Neurology. ;64(3):406-407.

-Moulder JE, Foster KR, Erdreich LS, McNamee JP. (2006). Mobile phones, mobile phone base stations and cancer. Int. J. Radiation Biol. 81: 189 - 203. [PubMed: 16019928].

-Mueller BA, Newton K, Holly EA, Preston-Martin S. (2001). Residential water source and the risk of childhood brain tumors. Environ Health Perspect. 109(6): 551–556. [PubMed: 11445506].

-Mullins ME. (2006). MR spectroscopy: truly molecular imaging; past, present and future. *Neuroimaging Clin N Am* 16:605-618.

-Murphy PS, Viviers L, Abson C, Rowland IJ, Brada M, Leach MO, Dzik-Jurasz AS. 2004. Monitoring temozolomide treatment of low-grade glioma with proton magnetic resonance spectroscopy. Br J Cancer.; 90: 781-786.

-Nandigam, Kaveer, Laszlo L. Mechtler, and James G. Smirniotopoulos(2014). "Neuroimaging of neurocutaneous diseases." *Neurologic clinics* 32.1: 159-192.

-Nagae-Poetscher LM, Bonekamp D, Barker PB, Brant LJ, Kaufmann WE, Horská A. (2004). Asymmetry and gender effect in functionally lateralized cortical regions: a proton MRS imaging study. *J Magn Reson Imaging* 19:27-33Nelson,

Sarah J. "Multivoxel magnetic resonance spectroscopy of brain Tumors1." Molecular Cancer Therapeutics 2.5 (2003): 497-507.

-Norton, Neil S. (2016)Netter's Head and Neck Anatomy for Dentistry E-Book. Elsevier Health Sciences.

-Panigrahy, A., Krieger, M. D., Gonzalez-Gomez, I., Liu, X., McComb, J. G., Finlay, J. L., ... & Blüml, S. (2006). Quantitative short echo time 1H-MR spectroscopy of untreated pediatric brain tumors: preoperative diagnosis and characterization. American journal of neuroradiology, 27(3), 560-572.

-Pantel, K., Alix-Panabières, C., & Riethdorf, S. (2009). Cancer micrometastases. Nature reviews Clinical oncology, 6(6), 339-351.

-Parizel PM, Tanghe H, Hofman PAM. Magnetic resonance imaging of the brain. In: Reimer P, Parizel PM, Stichnoth F-A (eds) 2003: Clinical MR Imaging, 2nd edition. Springer-Verlag Berlin,: 77-146.

-Posse S, DeCarli C, Le Bihan D (1994) Three-dimensional echoplanar MR spectroscopic imaging at short echo times in the human brain. *Radiology* 192:733–738.

-Pouwels PJ, Frahm J. (1998). Regional metabolite concentrations in human brain as determined by quantitative localized proton MRS. *Magn Reson Med* 39:53-60.

-Rabinov JD, Lee PL, Barker FG, Louis DN, Harsh GR, Cosgrove GR, Chiocca EA, Thornton AF, Loeffler JS, Henson JW, Gonzalez RG. (2002). In vivo 3-T MR spectroscopy in the distinction of recurrent glioma versus radiation effects: initial experience. *Radiology*. Dec;225(3):871-9.

-Rijpkema M, Schuuring J, van der Meulen Y, van der Graaf M, Bernsen H, Boerman R, van der Kogel A, Heerschap A. (2003). Characterization of oligodendrogliomas using short echo time 1H MR spectroscopic imaging. *NMR Biomed*. Feb;16(1):12-8.

-Salih, F. (2015). Brain Tumors among Sudanese Patients (A histopathological Study) (Doctoral dissertation, UOFK).

-Schneider, Katherine A. (2011)Counseling about cancer: Strategies for genetic counseling. John Wiley & Sons.

-Schwartz, Jeffrey M., and Sharon Begley.(2009) The mind and the brain. Springer Science & Business Media.

-Shah N, Sattar A, Benanti M, Hollander S, Cheuck L.(2006) Magnetic resonance spectroscopy as an imaging tool for cancer: A review of the literature. J Am Osteopath Assoc.;106(1):23-27.

-Sharma P, Brown S, Walter G, Santra S, Moudgil B. Nanoparticles for bioimaging. Adv Colloid Interface Sci. 2006; 123-126: 471- 485.

-Sibtain, N. A., F. A. Howe, and D. E. Saunders. (2007) "The clinical value of proton magnetic resonance spectroscopy in adult brain tumours." *Clinical radiology*62.2:109-119.

-Siegel, Rebecca L., Kimberly D. Miller, and Ahmedin Jemal.(2015) "Cancer statistics." *CA: a cancer journal for clinicians* 65.1:5-29.

-Šimundić, Ana-Maria. "Measures of diagnostic accuracy: basic definitions." *Medical and biological sciences* 22.4 (2008): 61-65.

-Smith EA, Carlos RC, Junck LR, Tsien CI, Elias A, Sundgren PC. (2009). Developing a clinical decision model: MR spectroscopy to differentiate between recurrent tumor and radiation change in patients with new contrast-enhancing lesions. *AJR Am J Roentgenol.* Feb;192(2):W45-52.

-Soares DP, Law M. (2009). Magnetic resonance spectroscopy of the brain: review of metabolites and clinical applications. *Clin Radiol* 64:12-21.

-Soher BJ, van Zijl PC, Duyn JH, Barker PB. (1996). Quantitative proton MR spectroscopic imaging of the human brain. *Magn Reson Med* 35:356-363.

-Spampinato MV, Smith JK, Kwock L, Ewend M, Grimme JD, Camacho DL, Castillo M. (2007). Cerebral blood volume measurements and proton MR spectroscopy in grading of oligodendroglial tumors. *AJR Am J Roentgenol*. Jan;188(1):204-12.

-Srinivasan R, Sailasuta N, Hurd R, Nelson S & Pelletier D. (2005). Evidence of elevated glutamate in multiple sclerosis using magnetic resonance spectroscopy at 3 T. *Brain.* 128(Pt 5):1016-25.

-Stadlbauer A, Gruber S, Nimsky C, Fahlbusch R, Hammen T, Buslei R, Tomandl B, Moser E, Ganslandt O. (2006). Preoperative grading of gliomas by using metabolite quantification with high-spatial-resolution proton MR spectroscopic imaging. *Radiology.* Mar;238(3):958-69. Epub 2006 Jan 19.

-Steindorf K, Schlehofer B, Becher H, Hornig G, Wahrendorf J. (1994). Nitrate in drinking water. A case control study on primary brain tumors with an embedded drinking water survey in Germany. Int. J. Epidemiology. 23(3):451–457. [PubMed: 7960368].

-Stefan Lonn, Lars Klaeboe, Per Hall, Tiit Mathiesen, Anssi Auvinen, Helle C.

Christensen, Christoffer Johansen,Tiina Salminen, Tore Tynes and Maria Feychting. (2004). Incidence trends of adult primary intracerebral tumors in four nordic countries. Int. J. Cancer. 108, 450 – 455. DOI 10.1002/ijc.11578.

-Sun T, Warrington NM, Luo J, Brooks MD, Dahiya S, Snyder SC, Sengupta R, Rubin JB. (2014).Sexually dimorphic RB inactivation underlies mesenchymal glioblastoma prevalence in males. J. Clin. Invest. 124(9): 4123-33. DOI: 10.1172/JCI71048.

-Taghipour Zahir SH, Rezaei sadrabadi M, Dehghani F. (2011). Evaluation of Diagnostic Value of CT Scan and MRI in Brain Tumors and Comparison with Biopsy. Iranian Journal of Pediatric Hematology Oncology Vol. 1(4), P: 121-125.

-Taillibert S, Chodkiewicz C, Laigle-Donadey F, Napolitano M, Cartalat-Carel S, Sanson M. (2006). Gliomatosis cerebri: a review of 296 cases from the ANOCEF database and the literature. *J Neurooncol*. Jan;76(2):201-5

-Tedeschi G, Lundbom N, Raman R, Bonavita S, Duyn JH, Alger JR, Di Chiro G. (1997). Increased choline signal coinciding with malignant degeneration of cerebral gliomas: a serial proton magnetic resonance spectroscopy imaging study. *J Neurosurg.* Oct;87(4):516-24.

-Tobin, M. K., Geraghty, J. R., Engelhard, H. H., Linninger, A. A., & Mehta, A. I. (2015). Intramedullary spinal cord tumors: a review of current and future treatment strategies. *Neurosurgical focus*, *39*(2), E14.

-Van der Graaf M. (2010). In vivo magnetic resonance spectroscopy: basic methodology and clinical applications. *Eur Biophys J* 39:527-540.

-Van der Knaap, MS & Valk, J. (2005). *Magnetic Resonance of Myelin Disorders* (3rd edition), Springer, ISBN 13:9783540222866, Heidelberg, Germany.

-Varho T, Komu M, Sonninen P, Holopainen I, Nyman S, Manner T, Sillanpää M, Aula P, Lundbom N. (1999). A new metabolite contributing to N-acetyl signal in 1H MRS of the brain in Salla disease. *Neurology*. May 12;52(8):1668-72.

-Vermathen P, Laxer KD, Matson GB, Weiner MW. (2000). Hippocampal structures: anteroposterior N-acetylaspartate differences in patients with epilepsy and control subjects as shown with proton MR spectroscopic imaging. *Radiology* 214:403-410.

-Vuori K, Kankaanranta L, Häkkinen AM, Gaily E, Valanne L, Granström ML, Joensuu H, Blomstedt G, Paetau A & Lundbom N.(2004). Low-grade gliomas and focal cortical developmental malformations: differentiation with proton MR spectroscopy. *Radiology*. 230(3):703-8.

-Wang, Q., Zhang, H., Zhang, J., Wu, C., Zhu, W., Li, F., ... & Xu, B. (2016). The diagnostic performance of magnetic resonance spectroscopy in differentiating high-from low-grade gliomas: a systematic review and meta-analysis. *European radiology*, *26*(8), 2670-2684.

-Wang W, Hu Y, Lu P, Li Y, Chen Y, et al. (2014) Evaluation of the Diagnostic Performance of Magnetic Resonance Spectroscopy in Brain Tumors: A Systematic Review and Meta-Analysis. PLoS ONE 9(11): e112577. DOI:10.1371/journal.pone.0112577.

-Wilson J.L, I.F. Mosely. (1978). Diagnostic approach to cerebellar lesions.

Neuroradiol. 4: 250-258.

-Wrensch, M., Minn, Y., Chew, T., Bondy, M., & Berger, M. S. (2002). Epidemiology of primary brain tumors: current concepts and review of the literature. Neuro-oncology. 4(4): 278-299.

-Weybright P, Sundgren PC, Maly P, Hassan DG, Nan B, Rohrer S, Junck L. (2005). Differentiation between brain tumor recurrence and radiation injury using MR spectroscopy. *AJR Am J Roentgenol*. Dec;185(6):1471-6.

-Xu M, See SJ, Ng WH, Arul E, Back MF, Yeo TT, Lim CC. (2005). Comparison of magnetic resonance spectroscopy and perfusion-weighted imaging in presurgical grading of oligodendroglial tumors. *Neurosurgery*. May;56(5):919-26; discussion 919-26.

-Yun Zhu, Peizhong Peter Wang, Jing Zhao, Roger Green, Zhuoyu Sun, Barbara Roebothan, Josh Squires, Sharon Buehler, Elizabeth Dicks, Jinhui Zhao, Michelle Cotterchio, Peter T. Campbell, Meera Jain, Patrick S. Parfrey, and John R. Mclaughlin. (2014). Dietary N-nitroso compounds and risk of colorectal cancer: a case-control study in Newfoundland and Labrador and Ontario, Canada. Br. J. Nutr. 28; 111(6): 1109 - 1117. DOI: 10.1017/S0007114513003462.

-Zeng QS, Li CF, Liu H, Zhen JH, Feng DC. (2007). Distinction between recurrent glioma and radiation injury using magnetic resonance spectroscopy in combination with diffusion-weighted imaging. *Int. J. Radiat Oncol Biol Phys*. May 1;68(1):151-8. Epub 2007 Feb 7.

-Zhuoyu Sun, Barbara Roebothan, Josh Squires, Sharon Buehler, Elizabeth Dicks, Jinhui Zhao, Michelle Cotterchio, Peter T. Campbell, Meera Jain, Patrick S. Parfrey, and John R. Mclaughlin. (2014). Dietary N-nitroso compounds and risk of

colorectal cancer: a case-control study in Newfoundland and Labrador and Ontario, Canada. Br. J. Nutr. 28; 111(6): 1109 - 1117. DOI: 10.1017/S0007114513003462.

Appendix:

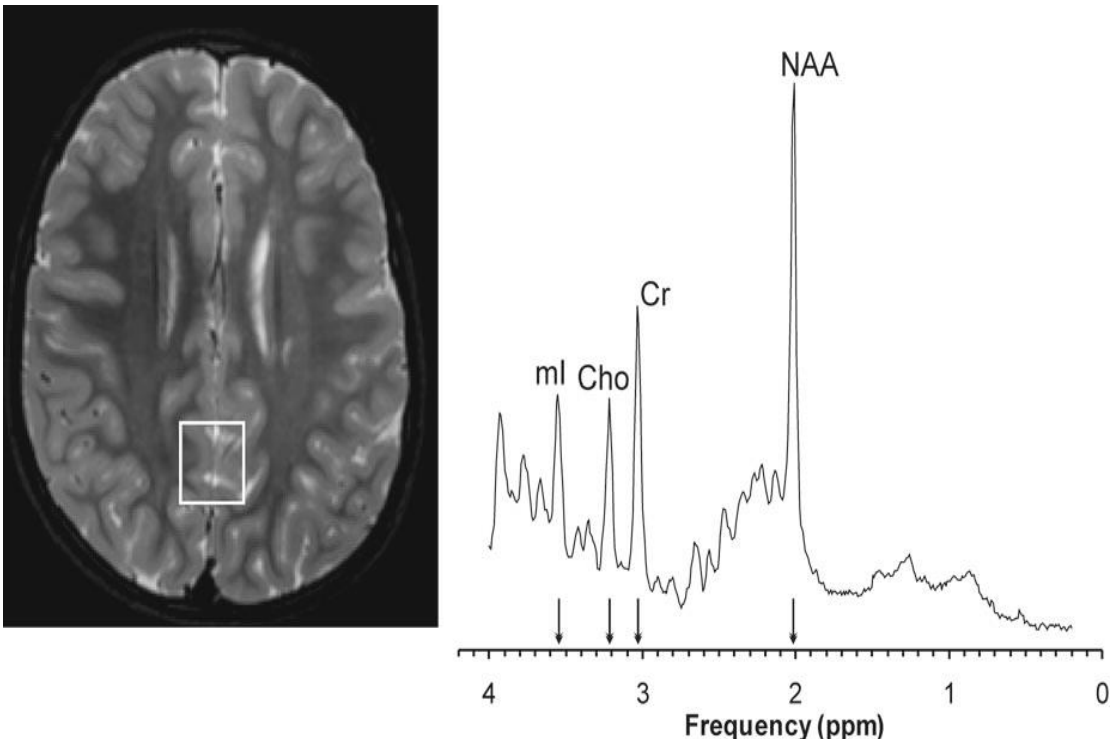

Image 1 : A spectrum is a frequency analysis (=Fourier transform) of the signal that is detected in an MR study. In this case, a normal gray matter spectrum, acquired from the region of interest (ROI) indicated by the box on the MR image, acquired with a standard PRESS sequence (TE 35ms) at 1.5T is shown. The height of a peak is equivalent to the strength of the signal. The position on the x -axis (or chemical shift axis) measures the chemical shift relative to a reference (tetramethylsilane (TMS) at 0 ppm) and can be used to identify chemicals. The water peak would be at 4.7 ppm. However, the water peak is suppressed in MRS sequences as it would be several orders of magnitude larger than any of the other peaks .

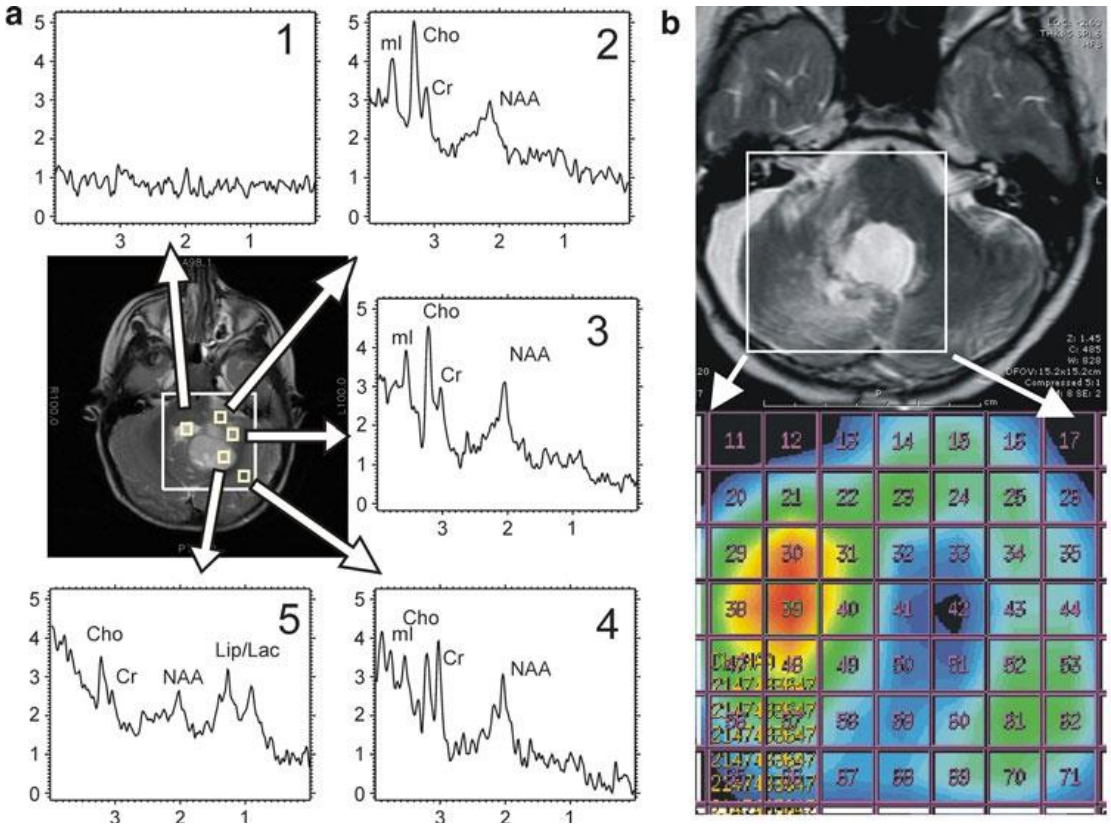

image 2 :(

a) 2D CSI of a 3-year-old boy with a posterior fossa astrocytoma. The data were acquired with a PRESS sequence with a repetition time (TR) of 1.0 s, TE = 35ms, fi eld of view = 160 bmm, 20 × 20 phase encoding steps, slice thickness = 8 mm, and two averages resulting in a nominal voxel resolution of 0.5 cc. Acquisition time was 13.3 min. The large boxes indicate the excited volume; smaller boxes indicate anatomical locations of individual spectra. (b) Shown is a 2D CSI of a child with a glioblastoma after radiation therapy. The box on the left image indicates the area from which spectra were acquired. Instead of displaying individual spectra, on the right, the results of the spectroscopy study are displayed as a color map. In this case, areas with increasing prominent choline relative to creatine (tCho/Cr) were colored hot yellow to red whereas areas with decreasing tCho/Cr are displayed in green and blue.

.

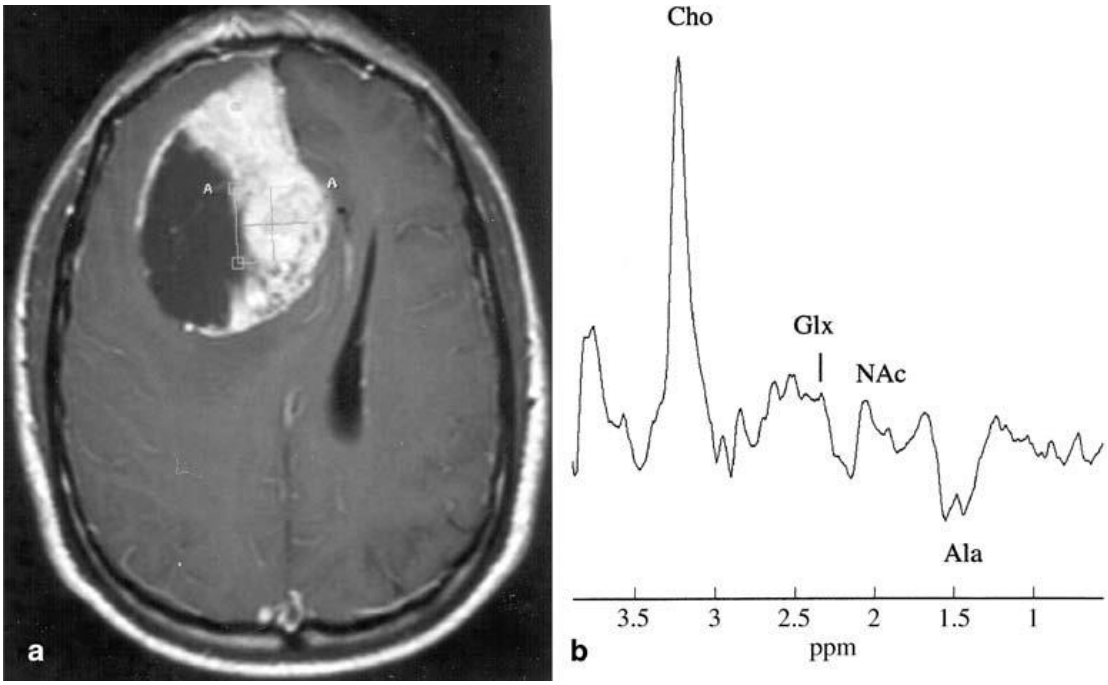

Image 3 :a, b Pathologically proven malignant meningioma in a 45-year-old man. a Axial T1-weighted contrast-enhanced MR image (TR 541 ms/TE 15 ms) shows a right frontal mixed tumour. There is a solid enhancing medial area and a lateral non-enhancing hypointense area suggesting cyst or necrosis. Peripheral enhancement is also seen. Extra-axial origin, as well as a diagnosis of meningioma, could not be confidently suggested from MRI alone. The 1H MRS was carried out in this case for obtaining additional information. The voxel position for 1H MRS is shown in the figure. A–A at the edges of the voxel are inerasable marks of the spectroscopic software used. b Localized 1H MRS (SE; TR/TE/no. of acquisitions: 2000 ms/136 ms/128) of the tumour voxel (line broadening= 1 Hz) shows a prominent inverted doublet centred at 1.47 ppm, attributable to Ala. A highly prominent resonance from Cho, as well as some amount of Glx, is also seen in the spectrum. The tumour was classified as meningioma by the empirical algorithm. This diagnosis satisfactorily matched with the final histological one.

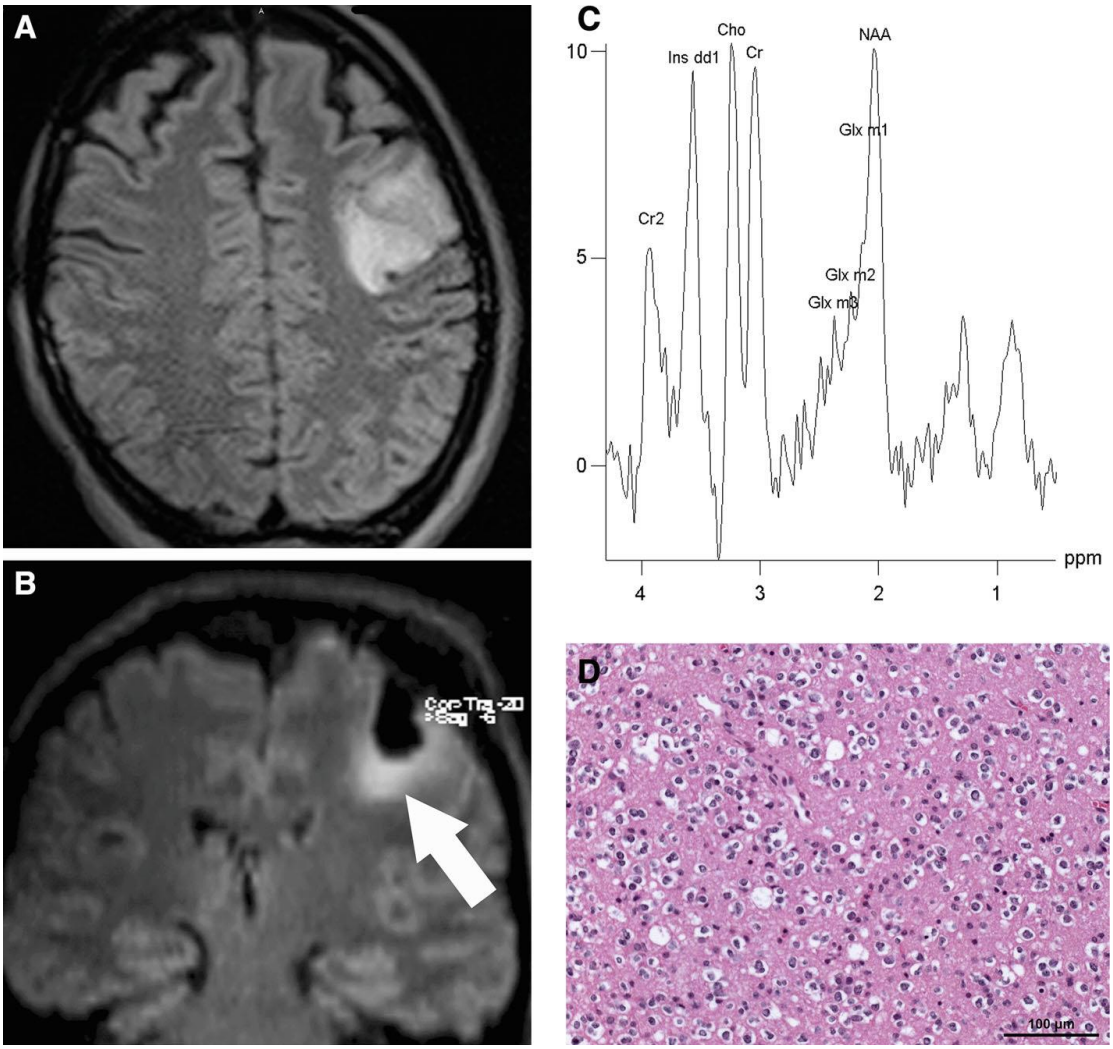

Image 4 :Axial T2-weighted FLAIR images of a 29-year-old female patient with hyperintense tumor on the left frontal lobe (a). The tumor was histologically proven to be low-grade glioma (oligodendroglioma WHO grade II). The intraoperative MRI (coronal T2-weighted FLAIR imaging) showed residual hyperintensity on the caudal resection margin (arrow in b). The performed spectroscopy showed slightly increased choline peak (c). The subsequently neuronavigation-guided sampled tissue at this site demonstrated moderate cell density, low nuclear pleomorphism and typical clear cytoplasm of tumor cells (hematoxylin and eosin), which corresponds to low-grade (oligodendroglioma WHO grade II) tumor parts (d). (Glx: combined signal from glutamate and glutamine).